


Cite this: *RSC Adv.*, 2024, 14, 17785

# Synthesis, docking and biological evaluation of purine-5-*N*-isosteres as anti-inflammatory agents†

Ahmed M. El-Saghier,<sup>id</sup>\*<sup>a</sup> Souhaila S. Enaili,<sup>ab</sup> Aly Abdou,<sup>id</sup><sup>a</sup> Amany M. Hamed<sup>a</sup> and Asmaa M. Kadry<sup>id</sup><sup>a</sup>

An operationally simple one-pot three-component and convenient synthesis method for a series of diverse purine analogues of 5-amino-7-(substituted)-*N*-(4-sulfamoylphenyl)-4,7-dihydro-[1,2,4]-triazolo[1,5-*a*] [1,3,5]triazine-2-carboxamide derivatives generated *in situ* via the reaction of 2-hydrazinyl-*N*-(4-sulfamoylphenyl)-2-thioxoacetamide, cyanoguanidine and a variety of aldehydes was achieved under green conditions. This experiment was conducted to evaluate the anti-inflammatory effect of the newly synthesized compounds using indomethacin as a reference medication; all compounds were tested for *in vitro* anti-inflammatory activity using the inhibition of albumin denaturation, RBC hemolysis technique and COX inhibition assay. The results showed that all evaluated compounds exhibited significant *in vitro* anti-inflammatory efficacy leading to excellently effective RBC membrane stabilization, inhibition of protein denaturation, and inhibition of COX enzymes when compared to those of indomethacin. At concentrations of 50, 100, 200, and 300  $\mu\text{g ml}^{-1}$ , these compounds decreased COX-1 and COX-2 activities more than indomethacin and have  $\text{IC}_{50}$  values in the range of 40.04–87.29  $\mu\text{g ml}^{-1}$  for COX-1 and 27.76–42.3  $\mu\text{g ml}^{-1}$  for COX-2 while indomethacin showed  $\text{IC}_{50} = 91.57$  for COX-1 and 42.66  $\mu\text{g ml}^{-1}$  for COX-2. The anti-inflammatory findings show the need for more investigation to define the properties underlying the evaluated compounds' anti-inflammatory abilities. The enzyme cyclooxygenase-2 (COX 2) (PDB ID: 5IKT) was docked with ten synthetic substances. With docking scores (*S*) of –8.82, –7.82, and –7.76  $\text{kcal mol}^{-1}$ , 7-furan triazolo-triazine (**4**), 7-(2-hydroxy phenyl) triazolo-triazine (**11**), and 7-(4-dimethylamino phenyl) triazolo-triazine (**12**) had the greatest binding affinities, respectively. Therefore, these substances have COX-2 (PDB ID: 5IKT) inhibitory capabilities and hence may be investigated for COX 2 targeting development. Furthermore, both the top-ranked compounds (**4** and **11**) and the standard indomethacin were subjected to DFT analysis. The HOMO – LUMO energy difference ( $\Delta E$ ) of the mentioned compounds was found to be less than that of indomethacin.

Received 22nd April 2024

Accepted 30th April 2024

DOI: 10.1039/d4ra02970d

rsc.li/rsc-advances

## 1. Introduction

When a damaging stimulus, trauma, or infection is present, the body responds with an intricate series of reactions known as inflammation. Under physiological circumstances, this response is advantageous to the host but chronic inflammation can cause serious host damage, tissue loss, and even organ failure due to the release of pathogenic mediators.<sup>1,2</sup> Pathologic hyper reactive inflammatory reactions are the outcome of reduced cytoprotective NRF2 cascade.<sup>3</sup>

Thus, to be able to prevent the onset of a number of persistent inflammatory conditions such as Alzheimer's disease, periodontitis, colitis, rheumatoid arthritis,

inflammatory bowel disease, septic shock, cardiovascular disease, and osteoporosis,<sup>4,5</sup> it is crucial for the host to discover mechanisms for regulating, avoiding, or reducing the release of inflammatory mediators in comparison with natural products.<sup>6</sup> Organic and medicinal chemistry efforts are ongoing to develop, synthesise, assess, and isolate substances with the potential to treat inflammation. These molecules are typically derived from heterocyclic compounds with sulfur or nitrogen atoms in their structures. Because they represent a significant class of both natural and synthetic compounds with a wide range of physicochemical characteristics and pharmacological actions, azaheterocycles are of increased interest.<sup>6,7</sup> Triazine derivatives are a particular class of heterocycles that contain nitrogen and have a wide range of properties, including a pain reliever, an antifungal, an anticancer, an antiprotozoal, and an antitubercular. They are consequently regarded as a crucial heterocycle framework for chemical pharmaceuticals.<sup>8</sup> The heterocycle purine, which contains nitrogen, is abundant in nature. In RNA and DNA, adenine and guanine are made of

<sup>a</sup>Chemistry Department, Faculty of Science, Sohag University, 282524, Sohag, Egypt. E-mail: el.saghier@science.sohag.edu.eg

<sup>b</sup>Chemistry Department, Faculty of Science, Al Zawiya University, Al Zawiya, Libya

† Electronic supplementary information (ESI) available. See DOI: <https://doi.org/10.1039/d4ra02970d>



these fundamental structures. Purine nucleotides (ATP, GTP, cAMP, cGMP, NAD, and FAD) work as co-factors, substrates, or mediators in the functioning of various proteins, which is primarily what attracts biological attention to them.<sup>9,10</sup> These proteins are thought to contain half of the targets that are most amenable to medication, primarily enzymes and receptors. For instance, protein kinases carry out the phosphorylation of ATP, while the cyclic nucleotide phosphodiesterase is involved in the hydrolysis of cAMP and cGMP.<sup>11,12</sup> The essential enzyme xanthine oxidase is involved in the breakdown of purines, while the ubiquitous purine nucleoside phosphorylase is essential for the purine salvage route. A very promising class of G-protein-coupled receptors (GPCRs) are adenosine receptors.<sup>13–15</sup>

Purine isosteres, a structurally similar heterocyclic system, saw parallel developments in chemistry and biology as a result of improvements in the purine motif-based design and development of drugs. They are suitable for the identification of innovative medicines focusing on purine-dependent enzymes and receptors to increase molecular diversity by employing different purine isosteres. There are many well-known medications with purine isostere core structures on the market, such as xanthine, hypoxanthine, theobromine, caffeine, uric acid, and isoguanine.<sup>14,15</sup>

The tubercidin deazapurines,<sup>16</sup> toyocamycin,<sup>17</sup> and sangivamycin<sup>18</sup> act as metabolite inhibitors and are employed as broad-spectrum antibiotics, which is also remarkable. Purine isosteres are the subject of considerable and ongoing research and development efforts, and one of the most promising avenues focuses on employing purine isosteres based on triazine.

Azolo-triazine systems in this category can be broadly classified as purine 5-*N*-isosteres because they contain a nitrogen atom in position 5 of the purine ring. As a result, the basic structure of this work focuses on certain areas of the compounds' medicinal features rather than how they relate to the heterocyclic system. Research on the triazolo-triazines and the deazapurines has been increasing.<sup>19,20</sup> In this paper, the authors highlight the significance of purine isosteres, specifically the 1,3,5-triazines, in medicinal chemistry by establishing a solid rationale for their research by explaining how these compounds target purine-binding proteins with therapeutic potential. Also, the importance of designing drugs with reduced side effects, particularly in the context of non-steroidal anti-inflammatory drugs (NSAIDs), is emphasized.

In accordance with a previous literature review, our focus in this work is synthesizing a novel purine analogue of 1,3,4-triazolo-1,3,5-triazines bearing sulfamoyl carboxamide moieties with a variety of substituted aryls at position 7 which are expected to have potential function as active pharmacophores against COX-2 enzyme because of the significance of isosteres systems as anti-inflammatory agents, and we further confirm it using a molecular docking technique.

## 2. Methodology

### 2.1. Chemistry

The melting point of every prepared target compound was calculated using the Fisher–John mechanical approach. Sigma-

Aldrich provided the chemicals and solvents needed for this investigation. The synthesized compounds' infrared ( $\nu$  cm<sup>-1</sup>) spectra were examined using the KBr technique, and a Bruker ADVANCE 400 MHz spectrometer was used to record the <sup>1</sup>H NMR ( $\delta$  ppm) and <sup>13</sup>CNMR spectra (Sohag University). A Vario El Fab-Nr elemental analyzer (Cairo University) was used to record elemental analyses.

#### 2.1.1. Synthesis of 5-amino-7-(substituted)-*N*-(4-sulfamoylphenyl)-4,7-dihydro-[1,2,4]-triazolo[1,5-*a*][1,3,5]triazine-2-carboxamidederivatives 4–13

**2.1.1.1 General procedure.** To a solution of 2-hydrazinyl-*N*-(4-sulfamoylphenyl)-2-thioxoacetamide (**1**) (0.001 mol), cyanoguanidine (**2**) (0.001 mol) and 0.001 mol of aldehyde derivatives (**3a–j**) in ethanol (15 ml) and HCl (0.001 mol, 1 ml) were added, and the reaction mixture was refluxed with stirring for about 3 h. The reaction was cooled, and the solid precipitate was collected by filtration and crystallized with ethanol.

**2.1.1.2 5-Amino-7-(furan-2-yl)-*N*-(4-sulfamoylphenyl)-4,7-dihydro-[1,2,4]-triazolo[1,5-*a*][1,3,5]triazine-2-carboxamide (**4**).** Greenish yellow solid, yield 89%. Mp. 212–214 °C. FT IR (KBr)  $\nu_{\max}$  cm<sup>-1</sup>: 3347, 3248, 3224 (2NH, 2NH<sub>2</sub>), 3142 (CH<sub>arom</sub>), 2924, 2756 (CH<sub>aliph</sub>), 1694 (C=O<sub>amide</sub>, st), 1667 (C=N) and 1159 (S=O, st). <sup>1</sup>H-NMR ( $\delta$  ppm): 11.28 (s, 1H, NH<sub>amide</sub>, exchangeable by D<sub>2</sub>O), 10.50 (s, 1H, NH<sub>triazine</sub>, exchangeable by D<sub>2</sub>O), 9.36 (s, 1H, CH<sub>triazole</sub>), 7.90–7.78 (m, 6H, 4H<sub>arom</sub> + NH<sub>2</sub>), 7.29–7.23 (m, 3H, NH<sub>2</sub> + 1CH<sub>furan</sub>), 6.46 (s, 2H, 2CH<sub>furan</sub>); <sup>13</sup>CNMR (DMSO-*d*<sub>6</sub>),  $\delta$  ppm: 158.89 (C=O), 153.23 (C–O), 147.99, 144.24, 141.53 (3C=N), 141.14, 139.30 (2C<sub>arom</sub>), 138.18 (CH–O), 126.92 (C–NH), 121.11, 120.50 (CH<sub>arom</sub>), 111.20, 108.23 (CH<sub>furan</sub>) and 67.11 (CH<sub>triazine</sub>). CF/MW: C<sub>15</sub>H<sub>14</sub>N<sub>8</sub>O<sub>4</sub>S/402; elemental analysis: calc./found: C, 44.77/44.80; H, 3.51/3.49; N, 27.85/27.79; S, 7.97/7.96%.

**2.1.1.3 5-Amino-*N*-(4-sulfamoylphenyl)-7-(*o*-tolyl)-4,7-dihydro-[1,2,4]-triazolo[1,5-*a*][1,3,5]triazine-2-carboxamide (**5**).** Yellow solid, yield 79%. Mp. 222–224 °C. FT IR (KBr)  $\nu_{\max}$  cm<sup>-1</sup>: 3390, 3334, 3253 (2NH, 2NH<sub>2</sub>), 3070 (CH<sub>arom</sub>), 2925, 2756 (CH<sub>aliph</sub>), 1685 (C=O<sub>amide</sub>, st), 1663 (C=N) and 1156 (S=O, st). <sup>1</sup>H-NMR ( $\delta$  ppm): 11.27 (s, 1H, NH<sub>amide</sub>), 10.49 (s, 1H, NH<sub>triazine</sub>), 9.36 (s, 1H, CH<sub>triazine</sub>), 7.89–7.77 (m, 6H, 4H<sub>arom</sub> + NH<sub>2</sub>), 7.45–7.24 (m, 6H, 4H<sub>arom</sub> + NH<sub>2</sub>), 2.34 (s, 3H, CH<sub>3</sub>); <sup>13</sup>CNMR (DMSO-*d*<sub>6</sub>),  $\delta$  ppm: 158.87 (C=O), 141.74, 141.18, 140.23 (3C=N), 139.45, 139.24, 137.87, 134.74 (4C<sub>arom</sub>), 131.75, 131.14 (2CH<sub>arom</sub>), 128.85, 126.83, 120.99, 120.22 (4CH<sub>arom</sub>), 72.11 (CH<sub>triazine</sub>) and 19.39 (CH<sub>3</sub>). CF/MW: C<sub>18</sub>H<sub>18</sub>N<sub>8</sub>O<sub>3</sub>S/426.46; elemental analysis: calc./found: C, 50.70/50.68; H, 4.25/4.20; N, 26.28/26.26; S, 7.52/7.48%.

**2.1.1.4 (*E*)-5-Amino-7-styryl-*N*-(4-sulfamoylphenyl)-4,7-dihydro-[1,2,4]-triazolo[1,5-*a*][1,3,5]triazine-2-carboxamide (**6**).** Dark yellow solid, yield 88%. Mp. > 300 °C. FT IR (KBr)  $\nu_{\max}$  cm<sup>-1</sup>: 3444, 3385, 3266, 3226 (2NH, 2NH<sub>2</sub>), 3070 (CH<sub>arom</sub>), 2926, 2857 (CH<sub>aliph</sub>), 1681 (C=O<sub>amide</sub>, st), 1664 (C=N) and 1160 (S=O, st). <sup>1</sup>H-NMR ( $\delta$  ppm): 11.28 (s, 1H, NH<sub>amide</sub>), 10.82 (s, 1H, NH<sub>triazine</sub>), 10.45 (s, 1H, CH<sub>triazine</sub>), 8.01–7.65 (m, 9H, NH<sub>2</sub> + 5H-arom + 2CH=), 7.37–7.25 (m, 6H, 4H-arom + NH<sub>2</sub>); <sup>13</sup>CNMR (DMSO-*d*<sub>6</sub>),  $\delta$  ppm: 157.10 (C=O), 156.17, 155.57, 154.90 (3C=N), 143.94, 141.25, 140.25 (3C<sub>arom</sub>), 135.94, 134.88 (CH<sub>arom</sub>), 131.67, 129.45 (2CH=), 128.36, 127.04, 121.00 (5CH<sub>arom</sub>) and 68.99 (CH<sub>triazine</sub>). CF/MW: C<sub>19</sub>H<sub>18</sub>N<sub>8</sub>O<sub>3</sub>S/438.47; elemental analysis:



calc./found: C, 52.05/52.00; H, 4.14/4.11; N, 25.56/25.53; S, 7.31/7.29%.

**2.1.1.5 5,5'-Diamino-N2,N2'-bis(4-sulfamoylphenyl)-4,4',7,7'-tetrahydro-[7,7'-bi[1,2,4]triazolo[1,5-a][1,3,5]triazine]-2,2'-dicarboxamide (7).** White solid, yield 84%. Mp. 228–230 °C. FT IR (KBr)  $\nu_{\max}$  cm<sup>-1</sup>: 3375, 3332, 3295 (2NH, 2NH<sub>2</sub>), 3070 (CH<sub>arom.</sub>), 2929, 2853 (CH<sub>aliph.</sub>), 1694 (C=O<sub>amide</sub>, st), 1663 (C=N) and 1160 (S=O, st). <sup>1</sup>H-NMR ( $\delta$  ppm): 11.30 (s, 1H, NH<sub>amide</sub>, exchangeable by D<sub>2</sub>O), 10.49 (s, 1H, NH<sub>triazine</sub>, exchangeable by D<sub>2</sub>O), 8.04–7.77 (m, 6H, NH<sub>2</sub> + 4H<sub>arom.</sub>), 7.30 (s, 2H, NH<sub>2</sub>), 5.55 (s, 1H, CH); <sup>13</sup>CNMR (DMSO-d<sub>6</sub>),  $\delta$  ppm: 159.45 (C=O), 158.61, 157.25, 155.22 (3C=N), 142.06, 139.88 (2C<sub>arom.</sub>), 127.04, 121.37 (CH<sub>arom.</sub>) and 56.11 (CH<sub>triazine</sub>). CF/MW: C<sub>22</sub>H<sub>22</sub>N<sub>16</sub>O<sub>6</sub>S<sub>2</sub>/670.64; elemental analysis: calc./found; C, 39.40/39.42; H, 3.31/3.29; N, 33.42/33.40; S, 9.56/9.55%.

**2.1.1.6 5-Amino-7-(2-chlorophenyl)-N-(4-sulfamoylphenyl)-4,7-dihydro-[1,2,4]-triazolo[1,5-a][1,3,5]triazine-2-carboxamide (8).** White solid, yield 84%. Mp. 220–222 °C. FT IR (KBr)  $\nu_{\max}$  cm<sup>-1</sup>: 3372, 3334, 3303, 3264 (2NH, 2NH<sub>2</sub>), 3070 (CH<sub>arom.</sub>), 2752, 2726 (CH<sub>aliph.</sub>), 1694 (C=O<sub>amide</sub>, st), 1666 (C=N) and 1160 (S=O, st). <sup>1</sup>H-NMR ( $\delta$  ppm): 11.51 (s, 1H, NH<sub>amide</sub>), 11.30 (s, 1H, NH<sub>triazine</sub>), 9.49 (s, 1H, CH<sub>triazine</sub>), 8.32 (s, 2H, NH<sub>2</sub>), 8.10–7.70 (m, 8H, H<sub>arom.</sub>), 7.31 (s, 2H, NH<sub>2</sub>); <sup>13</sup>CNMR (DMSO-d<sub>6</sub>),  $\delta$  ppm: 166.05 (C=O), 163.66 (C-Cl), 157.11, 155.41, 150.18 (3C=N), 141.20, 141.03, 140.52, 140.15 (4C<sub>arom.</sub>), 137.93, 131.44 (2CH<sub>arom.</sub>), 130.32, 127.05, 121.11 (CH<sub>arom.</sub>) and 69.08 (CH<sub>triazine</sub>). CF/MW: C<sub>17</sub>H<sub>15</sub>ClN<sub>8</sub>O<sub>3</sub>S/446.87; elemental analysis: calc./found: C, 45.69/45.70; H, 3.38/3.36; Cl, 7.93/7.0; N, 25.08/25.00; S, 7.17/7.15%.

**2.1.1.7 5-Amino-7-(4-methoxyphenyl)-N-(4-sulfamoylphenyl)-4,7-dihydro-[1,2,4]-triazolo[1,5-a][1,3,5]triazine-2-carboxamide (9).** Dark yellow solid, yield 71%. Mp. 254–256 °C. FT IR (KBr)  $\nu_{\max}$  cm<sup>-1</sup>: 3351, 3264, 3169 (2NH, 2NH<sub>2</sub>), 3070 (CH<sub>arom.</sub>), 2925, 2855 (CH<sub>aliph.</sub>), 1690 (C=O<sub>amide</sub>, st), 1681 (C=N) and 1161 (S=O, st). <sup>1</sup>H-NMR ( $\delta$  ppm): 11.26 (s, 1H, NH<sub>amide</sub>), 10.45 (s, 1H, NH<sub>triazine</sub>), 9.22 (s, 1H, CH<sub>triazine</sub>), 7.91 (s, 2H, NH<sub>2</sub>), 7.81–7.24 (m, 8H, H<sub>arom.</sub>), 6.88 (s, 2H, NH<sub>2</sub>), 3.81 (s, 3H, OCH<sub>3</sub>); <sup>13</sup>CNMR (DMSO-d<sub>6</sub>),  $\delta$  ppm: 159.16 (C=O), 157.82, 155.87, 153.86 (3C=N), 141.78, 141.25, 140.19, 139.18 (4C<sub>arom.</sub>), 128.09, 127.03, 120.63, 120.21 (CH<sub>arom.</sub>), 69.28 (CH<sub>triazine</sub>) and 56.49 (OCH<sub>3</sub>). CF/MW: C<sub>18</sub>H<sub>18</sub>N<sub>8</sub>O<sub>4</sub>S/442.45; elemental analysis: calc./found: C, 48.86/48.84; H, 4.10/4.09; N, 25.33/25.31; S, 7.25/7.22%.

**2.1.1.8 5-Amino-7-(naphthalen-1-yl)-N-(4-sulfamoylphenyl)-4,7-dihydro-[1,2,4]-triazolo[1,5-a][1,3,5]triazine-2-carboxamide (10).** White solid, yield 86%. Mp. 202–204 °C. FT IR (KBr)  $\nu_{\max}$  cm<sup>-1</sup>: 3442, 3398, 3378 (2NH, 2NH<sub>2</sub>), 3070 (CH<sub>arom.</sub>), 2925, 2855 (CH<sub>aliph.</sub>), 1690 (C=O<sub>amide</sub>, st), 1663 (C=N) and 1152 (S=O, st). <sup>1</sup>H-NMR ( $\delta$  ppm): 11.28 (s, 1H, NH<sub>amide</sub>, exchangeable by D<sub>2</sub>O), 10.54 (s, 1H, NH<sub>triazine</sub>, exchangeable by D<sub>2</sub>O), 9.54 (s, 1H, CH<sub>triazine</sub>), 8.22–7.24 (m, 15H, 2NH<sub>2</sub> + 11H<sub>arom.</sub>); <sup>13</sup>CNMR (DMSO-d<sub>6</sub>),  $\delta$  ppm: 159.02 (C=O), 141.74, 140.98, 139.26 (3C=N), 138.58, 136.66, 134.04, 132.62, 131.19 (5C<sub>arom.</sub>), 129.47, 126.93, 125.94, 121.14, 120.24 (CH<sub>arom.</sub>) and 71.79 (CH<sub>triazine</sub>). CF/MW: C<sub>21</sub>H<sub>18</sub>N<sub>8</sub>O<sub>3</sub>S/462.49; elemental analysis: calc./found: C, 54.54/54.55; H, 3.92/3.89; N, 24.23/24.20; S, 6.93/6.90%.

**2.1.1.9 5-Amino-7-(2-hydroxyphenyl)-N-(4-sulfamoylphenyl)-4,7-dihydro-[1,2,4]-triazolo[1,5-a][1,3,5]triazine-2-carboxamide**

**(11).** Canary yellow solid, yield 90%. Mp. 250–252 °C. FT IR (KBr)  $\nu_{\max}$  cm<sup>-1</sup>: 3468 (OH), 3351, 3264, 3168 (2NH, 2NH<sub>2</sub>), 3070 (CH<sub>arom.</sub>), 2825, 2725 (CH<sub>aliph.</sub>), 1692 (C=O<sub>amide</sub>, st), 1663 (C=N) and 1161 (S=O, st). <sup>1</sup>H-NMR ( $\delta$  ppm): 11.27 (s, 1H, NH<sub>amide</sub>), 10.45 (s, 1H, NH<sub>triazine</sub>), 9.93 (br, 1H, OH), 9.20 (s, 1H, CH<sub>triazine</sub>), 8.17 (s, 2H, NH<sub>2</sub>), 8.01–7.23 (m, 8H, H<sub>arom.</sub>), 6.88 (s, 2H, NH<sub>2</sub>); <sup>13</sup>CNMR (DMSO-d<sub>6</sub>),  $\delta$  ppm: 159.03 (C=O), 157.15, 155.74, 153.82 (3C=N), 140.82, 140.24, 139.18, 133.68 (4C<sub>arom.</sub>), 127.03, 120.99, 120.23, 117.02, 115.77 (CH<sub>arom.</sub>), 68.96 (CH<sub>triazine</sub>). CF/MW: C<sub>17</sub>H<sub>16</sub>N<sub>8</sub>O<sub>4</sub>S/428.43; elemental analysis: calc./found: C, 47.66/47.60; H, 3.76/3.70; N, 26.16/26.00; S, 7.48/7.41%.

**2.1.1.10 5-Amino-7-(4-(dimethyl amino) phenyl)-N-(4-sulfamoylphenyl)-4,7-dihydro-[1,2,4]-triazolo[1,5-a][1,3,5]triazine-2-carboxamide (12).** Red solid, yield 88%. Mp. 200–202 °C. FT IR (KBr)  $\nu_{\max}$  cm<sup>-1</sup>: 3346, 3306, 3259, 3172 (2NH, 2NH<sub>2</sub>), 3055 (CH<sub>arom.</sub>), 2926 (CH<sub>aliph.</sub>), 1693 (C=O<sub>amide</sub>, st), 1640 (C=N) and 1157 (S=O, st). <sup>1</sup>H-NMR ( $\delta$  ppm): 11.34 (s, 1H, NH<sub>amide</sub>), 10.44 (s, 1H, NH<sub>triazine</sub>), 9.70 (s, 1H, CH<sub>triazine</sub>), 8.21 (s, 2H, NH<sub>2</sub>), 8.01–7.99 (m, 8H, H<sub>arom.</sub>), 7.44 (s, 2H, NH<sub>2</sub>), 3.10–3.05 (s, 6H, 2CH<sub>3</sub>); <sup>13</sup>CNMR (DMSO-d<sub>6</sub>),  $\delta$  ppm: 158.97 (C=O), 156.14, 154.96, 152.83 (3C=N), 141.80, 140.86, 140.60, 131.99 (4C<sub>arom.</sub>), 127.82, 127.05, 121.06, 120.29 (CH<sub>arom.</sub>), 63.30 (CH<sub>triazine</sub>), 18.75 and 14.40 (2CH<sub>3</sub>). CF/MW: C<sub>19</sub>H<sub>21</sub>N<sub>9</sub>O<sub>3</sub>S/455.50; elemental analysis: calc./found: C, 50.10/50.11; H, 4.65/4.55; N, 27.68/27.65; S, 7.04/7.00%.

**2.1.1.11 5-Amino-7-(3-hydroxyphenyl)-N-(4-sulfamoylphenyl)-4,7-dihydro-[1,2,4]-triazolo[1,5-a][1,3,5]triazine-2-carboxamide (13).** White solid, yield 74%. Mp. 252–254 °C. FT IR (KBr)  $\nu_{\max}$  cm<sup>-1</sup>: 3381 (OH), 3380, 3332, 3290, 3202 (2NH, NH<sub>2</sub>), 3106 (CH<sub>arom.</sub>), 2989, 2728 (CH<sub>aliph.</sub>), 1695 (C=O<sub>amide</sub>, st), 1664 (C=N), and 1162 (S=O, st). <sup>1</sup>H-NMR ( $\delta$  ppm): 11.31 (s, 1H, NH<sub>amide</sub>), 10.31 (s, 1H, NH<sub>triazine</sub>), 9.92 (s, 1H, OH), 9.22 (s, 1H, CH<sub>triazine</sub>), 8.06 (s, 2H, NH<sub>2</sub>), 7.99–7.84 (m, 8H, H<sub>arom.</sub>), 7.30 (s, 2H, NH<sub>2</sub>); <sup>13</sup>CNMR (DMSO-d<sub>6</sub>),  $\delta$  ppm: 159.41 (C=O), 158.41, 157.08, 155.33 (3C=N), 141.00, 140.27, 138.40, 138.14 (4C<sub>arom.</sub>), 137.93, 131.12 (2CH<sub>arom.</sub>), 130.71, 127.04, 121.03, 119.70 (CH<sub>arom.</sub>), and 63.22 (CH<sub>triazine</sub>). CF/MW: C<sub>17</sub>H<sub>16</sub>N<sub>8</sub>O<sub>4</sub>S/428.43; elemental analysis: calc./found: C, 47.66/47.68; H, 3.76/3.71; N, 26.16/26.11; S, 7.48/7.50%.

## 2.2. Biological evaluation

Three adult male Wistar rats (age 10–12 weeks, 180–200 g) were housed in a 12 h dark/light cycle animal facility with controlled temperature (20–25 °C) and humidity (40–70%). Food and water were given ad libitum throughout the study.<sup>21</sup>

A common protective response to tissue damage caused by physical trauma, toxic chemicals, or microbiological agents is inflammation. It is also the localized defense mechanism of living mammalian tissue against pathogens.<sup>22</sup> In the current work, the synthesized compounds' *in vitro* anti-inflammatory activity was evaluated by following methods.

**2.2.1. Inhibition of protein denaturation method.** The 5 ml reaction mixture also included 2.8 ml of buffer phosphate solution (pH 6.4), 0.2 ml of egg albumin, and 2 ml of the synthesized compound at concentrations of 50, 100, 200, and 300  $\mu$ g ml<sup>-1</sup>. In the standard solution, indomethacin was

utilized rather than a synthetic compound. Instead of the synthetic chemical solution, pure water was utilized in the control solution. These solutions were heated for five minutes at 70 °C after a 15-minute incubation period at 37 °C. The solutions' absorbance at 660 nm was assessed once they had warmed to room temperature. The test was performed three times, and, using the following formula, the percentage inhibition of protein denaturation was determined.

$$\% \text{Inhibition} = \frac{(\text{absorbance control} - \text{absorbance sample})}{(\text{absorbance control})} \times 100$$

The IC<sub>50</sub> values of the synthesized compounds and the standard were also calculated.

**2.2.2. Membrane stabilizing activity.**<sup>23</sup> Preparation of erythrocyte suspension: whole blood was obtained with heparinized syringes from healthy rats. The blood was washed three times with isotonic buffered solution (10 mM sodium phosphate buffer, pH 7.4). The buffer solution contained 0.2 g of NaH<sub>2</sub>PO<sub>4</sub>, 1.15 g of Na<sub>2</sub>HPO<sub>4</sub>, and 9 g of NaCl in one liter of distilled water. The blood was centrifuged each time for 10 minutes at 3000 rpm.

Hypotonic solution-induced rat erythrocyte hemolysis: the membrane stabilizing activities of the synthesized compounds were assessed using hypotonic solution-induced rat erythrocyte hemolysis.<sup>24</sup> The test sample consisted of a stock erythrocyte (RBC) suspension (0.5 ml) mixed with 5 ml of hypotonic solution in 10 mM sodium phosphate buffered saline (pH 7.4) containing the synthesized compound (50–300 µg ml<sup>−1</sup>) or indomethacin as a standard drug. The control sample consisted of 0.5 ml of RBC mixed with hypotonic buffered saline solution alone. The mixtures were incubated for 10 min at room temperature and centrifuged for 10 min at 3000 rpm, and the absorbance of the supernatant was measured at 540 nm. The percentage inhibition of hemolysis or membrane stabilization was calculated by the formula

$$\% \text{ Inhibition of hemolysis} = (\text{OD}_1 - \text{OD}_2 / \text{OD}_1) \times 100$$

where OD<sub>1</sub> is the optical density of the hypotonic-buffered saline solution alone and OD<sub>2</sub> is the optical density of the test sample in the hypotonic solution.

**2.2.3. In vitro COX inhibitory assay.** Thus far, the primary mode of action of NSAIDs has been COX inhibition. To learn more about the novel compounds' mechanism of action, it was found that compounds **4**, **5**, **8**, **11** and **12** might inhibit COX enzymes. A COX colorimetric inhibitor screening assay kit (Catalog No. 701050, Cayman Chemical Inc., Ann Arbor, MI, USA) was used to assess the inhibitory activity for COX-1 and COX-2. Briefly, the reaction mixture contained 150 µl of assay buffer, 10 µl of heme, 10 µl of enzyme (either COX-1 or COX-2), and 10 µl of compound (1 mg ml<sup>−1</sup>).<sup>25</sup> The test compounds were tested at concentrations of 50, 100 and 150 µg ml<sup>−1</sup> in a final volume of 1 ml. The test compounds **4**, **5**, **8**, **11** and **12** were tested against indomethacin (as a standard drug). The percent COX inhibition was calculated using following equation,

$$\text{COX inhibition activity (\%)} = (1 - T/C) \times 100$$

where *T* is the absorbance of the inhibitor well and *C* is the absorbance of the 100% initial activity without the inhibitor well.

The results were expressed in terms of IC<sub>50</sub> values and a COX-1/COX-2 selectivity index was calculated (Table 2).

**2.2.4. Statistical analysis.** Data were reported as mean ± SD, which was statistically analyzed using the Student's *t*-test and *p* < 0.001 vs. indomethacin was significant.

### 2.3. In silico analysis

The *in silico* pharmacokinetic analysis, including the Lipinski score and BOILED egg plot, was done using SWISS ADME.<sup>26</sup> Additionally, the *in silico* toxicity assessment was explored using OSIRIS Property Explorer.<sup>27</sup>

### 2.4. Molecular docking

The ten tested compounds (**4–13**) as ligands underwent molecular docking investigations using the MOE.<sup>25</sup> Using the MOE program's builder interface, 3D models of the target compounds (**4–13**) were generated.<sup>28,29</sup> The ligand preparation process was performed on the target compounds with the default features. The resulting database was then stored as an MDB file for the docking calculations. The atomic coordinates of the crystal structures of the studied enzyme, the structure of tolfenamic acid bound to human cyclooxygenase-2 with the Protein Data Bank (PDB) identification number 5IKT,<sup>30</sup> as receptor were obtained from the protein databank. The target enzyme structure was prepared by adding polar hydrogen atoms and removing water molecules, native ligands, and unwanted chains that were exposed.<sup>31,32</sup> The active site of 5IKT was docked with the ten compounds (**4–13**) and 30 conformations were generated for each compound.<sup>33</sup> The London G energy scoring function was used to evaluate the ligand–receptor complexes and the lowest scoring one was selected for further analysis of the binding orientations.<sup>25</sup>

The validity of the docking process was verified by a re-docking and superimposition strategy.<sup>34,35</sup> The native ligand of the 5IKT enzyme was extracted and then re-docked into the active site. The ESI† (S.I. Docking validation) shows the details of this process.

### 2.5. Density functional theory (DFT) exploration

DFT analyses play an essential role in the computation of molecular orbital characteristics.<sup>36,37</sup> In this framework, the top two compounds from the screening process (**4** and **11**) underwent a structure-based DFT analysis utilizing B3LYP<sup>38</sup> and a 6–311g(d, p) basis set<sup>39</sup> via G09w.<sup>40</sup> Comparative investigation between the highest occupied molecular orbital (HOMO) and lowest unoccupied molecular orbital (LUMO) energies was performed.<sup>41</sup>

## 3. Results and discussion

### 3.1. Chemistry

As part of our ongoing research into the synthesis of novel heterocycles,<sup>42–52</sup> we prepared in this article a new series of 5-

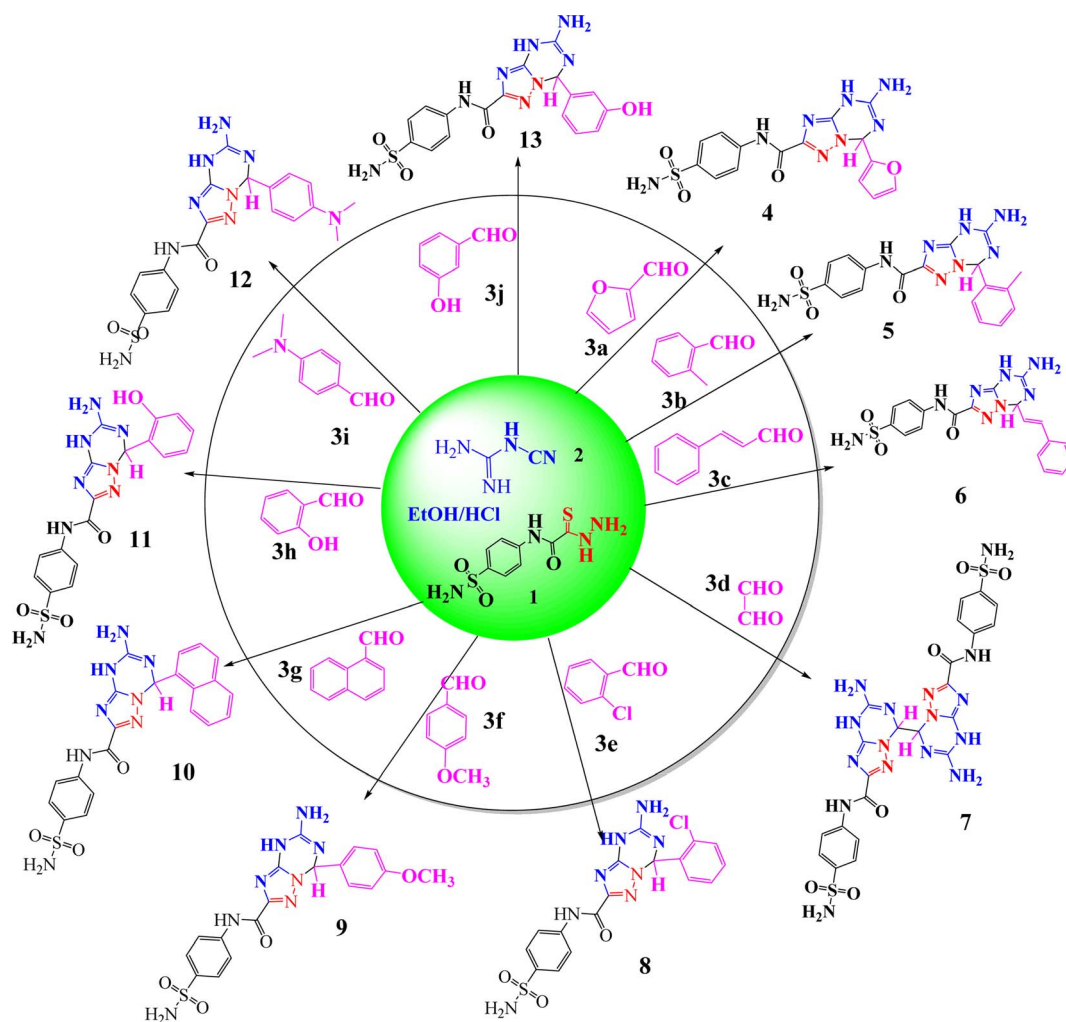


amino-7-(substituted)-*N*-(4-sulfamoylphenyl)-4,7-dihydro-[1,2,4]triazolo[1,5-*a*][1,3,5]triazine-2-carboxamidederivatives **4–13** by a new method, a smooth way, one-pot reaction, energy saving (at room temperature), low cost (without catalyst), short period (about 3 h), green solvent (EtOH) method, with high yields (79–93%) and no requirements for toxic chemicals, which follow the green synthesis rules. Thiocarbohydrazide **1** was allowed to react with cyanoguanidine **2** and various aldehydes **3a–3j**, namely, furfural, 2-methylbenzaldehyde, cinnamaldehyde, glyoxal, 2-chlorobenzaldehyde, 4-methoxybenzaldehyde, 1-naphthaldehyde, 2-hydroxybenzaldehyde, 4(*N,N*)-dimethyl benzaldehyde, and 3-hydroxybenzaldehyde. The one pot-reaction, three component system was applied in ethanol in the presence of a few drops of conc. HCl with stirring under reflux for 3 h, and the products **4–13** were precipitated on heat and separated by filtration (Scheme 1).

The reaction mechanism was assumed to occur *via* nucleophilic attack of the amino group of thiocarbohydrazide **1** at the cyano group of cyanoguanidine to afford a biguanidine intermediate, followed by nucleophilic attack of the NH of biguanidine at the carbon of thiocarbonyl (C=S), with elimination of

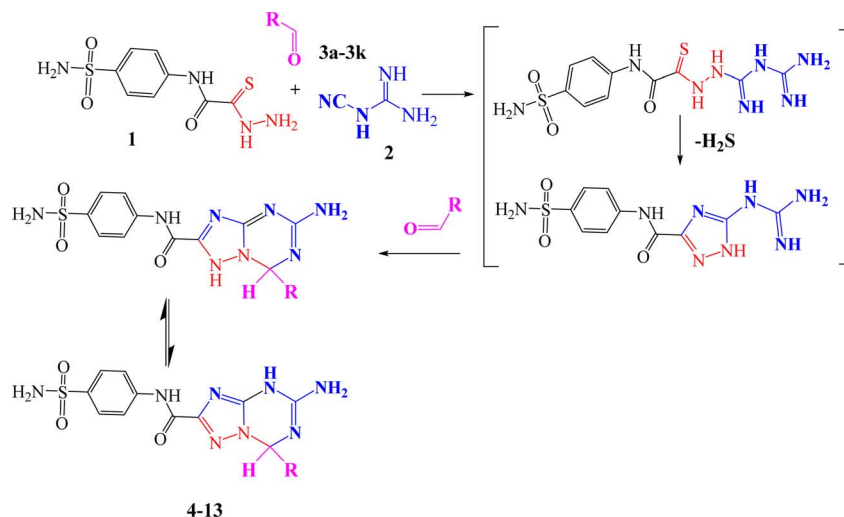
H<sub>2</sub>S (which is detected by paper dampened with lead acetate) to give 5-guanidino-*N*-(4-sulfamoylphenyl)-1*H*-1,2,4-triazole-3-carboxamide as an intermediate, and then nucleophilic attack of the NH of the triazole ring and NH of guanidine at the carbonyl group of the ketone with tautomerism to afford the desired triazolo-triazine compounds with elimination of water (Scheme 2).

1,3,4-Triazolo[1,3,5]triazine derivatives **4–13** were validated with physical and spectral analysis. The FT-IR spectra illustrated the appearance of the NH, NH<sub>2</sub> stretching band at 3395–3170 cm<sup>−1</sup>. Also, the disappearance of the C=S stretching band at 1287 cm<sup>−1</sup> and the C–S–C stretching band at 745 cm<sup>−1</sup> provided a definite sign that the triazolo-triazine system formed as a result of the reaction. In the <sup>1</sup>H NMR spectra, signals appeared at 11.62–11.08 (s, 1H, NH<sub>amide</sub>), 11.35–10.09 (s, NH<sub>triazine</sub>, exchangeable by D<sub>2</sub>O), 9.54–9.20 (s, 1H, CH<sub>triazine</sub>), 8.32–8.06 (s, 2H, NH<sub>2-triazine</sub>), 8.21–7.32 (m, CH<sub>aromatic</sub>), and 7.73–7.06 (s, 2H, NH<sub>2</sub>, exchangeable by D<sub>2</sub>O). The formations of triazolo-triazine compounds **4–13** were proved by a clear band at 76.90–63.30 ppm in the <sup>13</sup>C-NMR for CH<sub>triazine</sub>. The number of aliphatic and aromatic carbons confirmed the expected



**Scheme 1** Synthesis of 5-amino-7-(substituted)-*N*-(4-sulfamoylphenyl)-4,7-dihydro-[1,2,4]triazolo[1,5-*a*][1,3,5]triazine-2-carboxamide derivatives (**4–13**).





**Scheme 2** Reaction mechanism for 5-amino-7-(substituted)-*N*-(4-sulfamoylphenyl)-4,7-dihydro-[1,2,4]triazolo[1,5-*a*][1,3,5]triazine-2-carboxamidederivatives (**4–13**).

structure of the title compounds in the  $^{13}\text{C}$ -NMR spectrum. Finally, elemental analysis spectroscopic methods obtained information about the elemental compositions of the synthesized compounds.

In this work, the formed materials **4–13** were prepared under different conditions to detect the best method to give a high product yield, short time and green methodology with operational simplicity. Initially, we selected thiocarbohydrazide (**1**) to react with low-cost cyanoguanidine (**2**) and *p*-methoxybenzaldehyde (**3f**) as model substrates for the synthesis of 5-amino-7-(4-methoxyphenyl)-*N*-(4-sulfamoylphenyl)-4,7-dihydro-[1,2,4]triazolo[1,5-*a*][1,3,5]triazine-2-carboxamide (**9**) in a one pot method to optimize the reaction conditions, including the effects of type of acidic catalysis, solvent, temperature, time and yield. It is noted that the reaction rate went up when increasing the temperature; here, we recorded that no reaction happened at room temperature in the presence of  $\text{AlCl}_3$  (Table 1, entry 1). Using a different type of acidic catalysis with the same temperature and solvent enhanced compound **9**'s yield marginally to 43% (Table 1, entries 2–4); however, compound **9**'s yield marginally climbed to 44% with a shorter reaction time

(Table 1, entry 5). We also assessed how different solvent types affected the product yield during the same reaction time, finding that utilizing acid catalysis—such as HCl—significantly increased the yield of **9** in each of the solvents (Table 1, entries 6–8). Accordingly, using the same amount of HCl (1 equivalent), dioxane produced greater efficiency (60%) than acetonitrile (MeCN) (49%). We refluxed the reaction mixture under a shorter reaction time in order to further prepare triazolo-triazine **9** in a high yield (72%) (Table 1, entry 9). Remarkably, a yield of 79% of **9** was achieved with 1 equivalent of HCl refluxed for 3 hours (Table 1, entry 10). However, when HCl (2 equiv.) was added at the same reaction period, the reaction yield decreased to 74% (Table 1, entry 11). Compound **9** was synthesized using a one-pot method that adheres to green chemistry guidelines. Compound **9**'s elemental analysis and  $^{13}\text{C}$  NMR and  $^1\text{H}$  NMR data all agree well with the published data.

### 3.2. Biological evaluation

Many inflammatory illnesses can be treated with nonsteroidal anti-inflammatory medicines (NSAIDs, such as ibuprofen, aspirin, or naproxen), herbal supplements, such as curcumin,

**Table 1** Optimization of the reaction conditions for synthesis of compound **9** in one pot reaction

Entry	Acidic cat. (equiv.)	Temperature ( $^{\circ}\text{C}$ )	Solvent	Time (h)	Yield (%)
1	$\text{AlCl}_3$ (1.0)	RT	EtOH	18	Nil
2	Acetic acid (1.0)	Reflux	EtOH	7	37
3	Trifluoroacetic acid (1.0)	Reflux	EtOH	7	40
4	$\text{AlCl}_3$ (1.0)	Reflux	EtOH	7	43
5	$\text{AlCl}_3$ (2.0)	Reflux	EtOH	3	44
6	HCl (1.0)	RT	MeCN	18	49
7	HCl (1.0)	RT	Dioxane	18	60
8	HCl (1.0)	RT	EtOH	18	64
9	HCl (1.0)	Reflux	EtOH	7	72
10	HCl (1.0)	Reflux	EtOH	3	79
11	HCl (2.0)	Reflux	EtOH	3	74



capsaicin, and *Boswellia serrata*, and corticosteroids, such as prednisone, to reduce pain and fever.<sup>53</sup> However, 1–2% of NSAID users have been observed to have renal toxicity. Research indicates that using NSAIDs can result in renal failure, both acute and chronic.<sup>54</sup> Because of their toxic nature, NSAIDs cannot be used to treat inflammatory conditions. Therefore, it is crucial for pharmacological researchers to find new, affordable anti-inflammatory drugs with the fewest side effects possible. This is a difficult assignment for scientists.<sup>55</sup> Bioactive substances found in nature have long been utilized in traditional medicine to treat inflammatory conditions like pain, fever, arthritis, and migraines.<sup>56</sup> Heterocyclic compounds are widely distributed in nature and are vital to all living organisms. Numerous natural compounds, such as hormones, pigments, antibiotics, and vitamins, include them as fundamental subunits.<sup>57</sup> As a result, scientists have given them a lot of attention in their quest to create novel bioactive substances.<sup>58</sup> Nitrogen-containing heterocycles are a significant class and have made significant contributions to the field of medicinal chemistry research.<sup>59</sup>

Here, maximum denaturation of egg albumin was inhibited, and membrane stabilization of the RBC was achieved with synthesized compounds **4**, **5**, **8**, **11** and **12** at 50–300  $\mu\text{g ml}^{-1}$ . In the study of membrane stabilization activity, all the newly synthesized compounds protected the erythrocyte membrane significantly in a concentration dependent manner against lysis induced by hypotonic solution. Indomethacin at the same concentrations used as standards also offered significant ( $p < 0.05$ ) protection of the RBC membrane against the damaging effects induced by hypotonic solution. The membrane stabilization action and inhibitory effect of different concentrations of the synthesized compounds are presented in Fig. 1a and b. Both membrane stabilization activity and effect on protein denaturation contribute to the *in vitro* anti-inflammatory activity of all the synthesized compounds used in our study. Table 2 shows the  $\text{IC}_{50}$  values for the % inhibition of denaturing egg albumin and stabilizing synthetic compounds.

We evaluated the capacities of the synthesized compounds to inhibit COX-1 and COX-2 activities by an *in vitro* test and compared them to indomethacin (reference NSAID). As shown

in Fig. 2a and b, the synthesized compounds **4**, **5**, **8**, **11** and **12** induced a strong and dose-dependent inhibition. At 50, 100, and 150  $\mu\text{g ml}^{-1}$ , compounds **4**, **5**, **8**, **11** and **12** decreased COX-1 and COX-2 activities more than indomethacin. The results demonstrated that the newly synthesized compounds **4**, **5**, **8**, **11** and **12** have  $\text{IC}_{50}$  values in the range of 40.04–87.29  $\mu\text{g ml}^{-1}$  for COX-1 and 27.76–42.3  $\mu\text{g ml}^{-1}$  for COX-2, while the positive control indomethacin showed an  $\text{IC}_{50}$  of 91.57 for COX-1 and 42.66  $\mu\text{g ml}^{-1}$  for COX-2. It was noteworthy that compounds **4**, **5**, **8**, **11** and **12** showed higher inhibition for COX activities than indomethacin, with excellent selectivity indexes in the 1.44–2.07 range for the synthesized compounds (Table 3).

Because it is simple and accurate, the heat-induced egg albumin denaturation test is a commonly used method. This test was chosen because albumin protein denaturation produces antigens that set off type III hypersensitivity reactions that result in inflammation.<sup>60</sup> According to the findings of the current research, these synthetic compounds have a more potent anti-inflammatory impact than indomethacin. All the synthetic compounds inhibited the denaturation of egg albumin at 50, 100, 200, and 300  $\mu\text{g ml}^{-1}$ . The maximum activities were found in **4**, **5**, **8**, **11**, and **12** compared to the other studied compounds and indomethacin as a standard drugs.

In other ways, the *in vitro* membrane stabilization method indicated more effective, flexible, and useful. The study found that the synthesized compounds were more resistant to RBC lysis than the common drug indomethacin. Compounds **4**, **5**, **8**, **11** and **12** were able to prevent lysis more successfully than indomethacin because they have superior membrane stability and strong anti-inflammatory properties, while substances **6**, **7**, **9**, **10** and **13** are less effective at reducing inflammation than indomethacin. As a result of the relatively significant anti-inflammatory capabilities of synthesised compounds **4**, **5**, **8**, **11** and **12**, they displayed good potency against COX-1 and COX-2 enzymes in the COX inhibition assay. In comparison to indomethacin, the other investigated substances (**6**, **7**, **9**, **10** and **13**) demonstrated less inhibition against these enzymes. The results of the current investigation indicated that compounds **4**, **5**, **8**, **11** and **12** were the most effective at inhibiting both COX-1

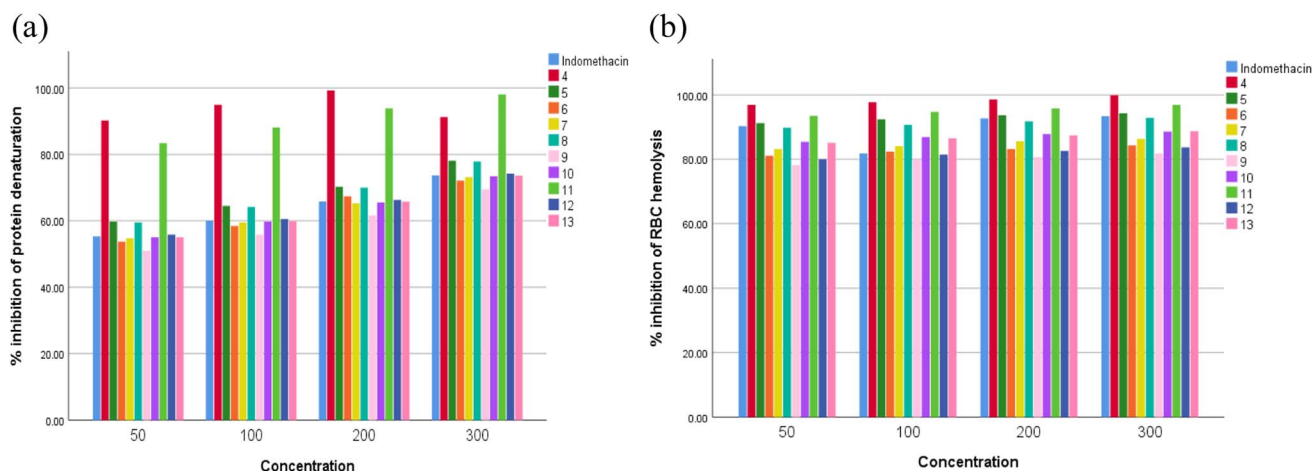


Fig. 1 *In vitro* anti-inflammatory activity by (a) protein denaturation and (b) membrane stabilization.



**Table 2** The anti-inflammatory impact of synthetic substances assessed *in vitro* using protein denaturation and hypotonic solution hemolysis techniques<sup>a</sup>

Compound code	Conc. ( $\mu\text{g ml}^{-1}$ )	Inhibition of protein denaturation (%)	IC <sub>50</sub> ( $\mu\text{g ml}^{-1}$ ) for protein denaturation	Inhibition of RBC hemolysis (%)	IC <sub>50</sub> ( $\mu\text{g ml}^{-1}$ ) for RBC hemolysis
Indomethacin	50	55.26	45.2	90.3	27.6
	100	60		91.8	
	200	65.78		92.7	
	300	73.68		93.4	
<b>4</b>	50	90.26	27.6	96.9	25.7
	100	95		97.7	
	200	99.2		98.6	
	300	91.3		99.9	
<b>5</b>	50	59.73	41.8	91.2	27.4
	100	64.47		92.4	
	200	70.26		93.7	
	300	78.15		94.3	
<b>6</b>	50	53.68	46.5	81.1	30.8
	100	58.42		82.4	
	200	67.36		83.2	
	300	72.1		84.3	
<b>7</b>	50	54.73	45.6	83.2	30
	100	59.47		84.1	
	200	65.26		85.6	
	300	73.15		86.3	
<b>8</b>	50	59.47	63.3	89.8	27.8
	100	64.21		90.7	
	200	70		91.8	
	300	77.89		92.9	
<b>9</b>	50	51.05	42	78.2	31.9
	100	55.78		79.8	
	200	61.57		80.6	
	300	69.47		81.8	
<b>10</b>	50	55	45.4	85.4	29.2
	100	59.73		86.9	
	200	65.52		87.8	
	300	73.42		88.6	
<b>11</b>	50	83.42	29.9	93.5	26.7
	100	88.15		94.7	
	200	93.94		95.8	
	300	98.15		96.9	
<b>12</b>	50	55.78	44.8	80	27.2
	100	60.52		81.4	
	200	66.31		82.6	
	300	74.21		83.7	
<b>13</b>	50	55	45.4	85.1	29.3
	100	59.83		86.5	
	200	65.72		87.4	
	300	73.62		88.7	

<sup>a</sup> IC<sub>50</sub> value is the compound concentration required to produce 50% inhibition. All the values are significant when compared to indomethacin ( $p < 0.05$ ).

and COX-2 at concentrations of 50, 100, and 150  $\mu\text{g ml}^{-1}$ . These derivatives may prove to be effective therapeutic molecules for inflammatory illnesses if further laboratory research is conducted on them.

### 3.3. *In silico* analysis

**3.3.1. Lipinski's analysis.** The results from the Lipinski's rule analysis<sup>61</sup> (Table 4), conducted using Swiss ADME<sup>26</sup> for the subject compounds, reveal a mix of adherence and violations. Lipinski's rule<sup>60</sup> suggests that for a compound to have good

oral bioavailability, it should generally have a molecular weight (MW) below 500  $\text{g mol}^{-1}$ , a log  $P$  (partition coefficient) less than 5, no more than 5 hydrogen bond donors (H donor), and no more than 10 hydrogen bond acceptors (H acceptor), along with fewer than 10 rotatable bonds. Among the compounds tested, compounds **4**, **5**, **6**, **8**, **9**, **10**, **11**, **12**, and **13** all adhere to Lipinski's rule, exhibiting properties conducive to good oral bioavailability. However, compound **7** fails to meet Lipinski's criteria, with violations in three areas: excessive molecular weight (670  $\text{g mol}^{-1}$ ), significantly negative log  $P$



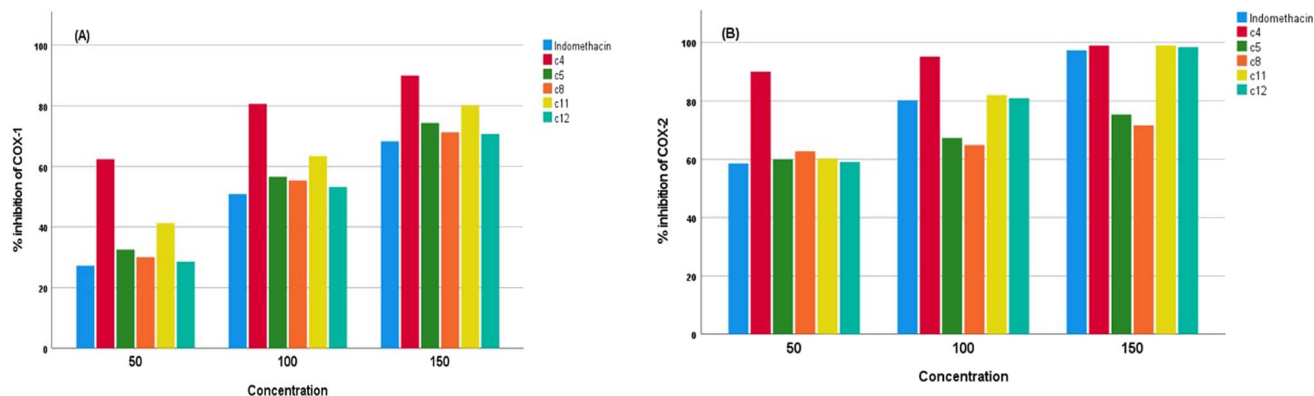


Fig. 2 Effect of synthesized compounds on (a) COX-1 activity and (b) COX-2 activity.

Table 3 Inhibitory effects of the synthesized compounds on COX enzymes

Compound code	Concentration ( $\mu\text{g ml}^{-1}$ )	Inhibition of COX-1 (%)	Inhibition of COX-2 (%)	COX-1 $\text{IC}_{50}$ ( $\mu\text{g ml}^{-1}$ )	COX-2 $\text{IC}_{50}$ ( $\mu\text{g ml}^{-1}$ )	Selectivity index
Indomethacin	50	$27.3 \pm 0.08$	$58.6 \pm 0.04$	91.57	42.66	2.14
	100	$50.88 \pm 0.1$	$80.2 \pm 0.05$			
	150	$68.24 \pm 0.2$	$97.3 \pm 0.03$			
4	50	$62.43 \pm 0.01$	$90.03 \pm 0.02$	40.04	27.76	1.44
	100	$80.64 \pm 0.01$	$95.11 \pm 0.01$			
	150	$90.02 \pm 0.02$	$98.92 \pm 0.02$			
5	50	$32.51 \pm 0.03$	$60.01 \pm 0.05$	76.89	41.65	1.84
	100	$56.64 \pm 0.01$	$67.25 \pm 0.02$			
	150	$74.32 \pm 0.03$	$75.31 \pm 0.01$			
8	50	$30.12 \pm 0.02$	$62.64 \pm 0.01$	83	39.91	2.07
	100	$55.41 \pm 0.05$	$64.78 \pm 0.01$			
	150	$71.23 \pm 0.05$	$71.61 \pm 0.01$			
11	50	$41.28 \pm 0.04$	$60.3 \pm 0.05$	60.56	41.45	1.46
	100	$63.43 \pm 0.04$	$81.99 \pm 0.01$			
	150	$80.12 \pm 0.03$	$98.97 \pm 0.06$			
12	50	$28.64 \pm 0.04$	$59.1 \pm 0.01$	87.29	42.3	2.06
	100	$53.24 \pm 0.03$	$80.98 \pm 0.02$			
	150	$70.68 \pm 0.04$	$98.4 \pm 0.02$			

(−2.153), and an excess of hydrogen bond acceptors (18) and donors (8). These results suggest that, while most of the compounds show promise for oral bioavailability, compound 7 may face challenges in this regard due to its physicochemical properties.

**3.3.2. BOILED-egg plot.** BOILED-Egg (Brain Or Intestinal Estimate D permeation method)<sup>62</sup> (Fig. 3) is a predictive model that works by calculating the polarity and lipophilicity of small molecules. Efficient and clear graphical outputs are obtained by converting the predictions of brain and intestinal absorption. A BOILED-Egg plot determines a drug's suitability during its development by depicting the statistical plots of gastrointestinal absorption and entry of small molecules into the brain. In the plot, the white region is for high probability of passive absorption by the gastrointestinal tract, and the yellow region (yolk) is for high probability of brain penetration. Yolk and white areas are not mutually exclusive. In addition, points are

colored in blue if they are predicted as active effluxes by P-gp (PGP+) and in red if predicted as a non-substrate of P-gp (PGP−).

**3.3.3. In silico toxicity using OSIRIS property explorer.** The results from the prediction of drug-likeness and toxicity using OSIRIS property explorer (Table 5) provide valuable insights into the pharmacodynamic and pharmacokinetic properties of the subject compounds. Overall, the majority of compounds show favorable properties with regard to mutagenicity, tumorigenicity, eye and skin irritation, and reproductive effects, as they are predicted to have no effects in these areas. However, compounds 10 and 12 are flagged for high tumorigenic potential in pharmacokinetics, indicating a potential concern for carcinogenicity. Moreover, compound 7 stands out with significantly negative scores in absorption and drug-likeness, suggesting potential challenges in its bioavailability and overall suitability as a drug candidate. Compound 10 also exhibits



Table 4 Lipinski's rule for the subject compounds by Swiss ADME

	MW (g mol <sup>-1</sup> )	Log <i>P</i> (<5)	Rotatable bonds	H acceptor (<10)	H donor (<5)	Lipinski's rule
4	402	0.058	4	4	10	Yes (1 violation)
5	426	0.773	4	9	4	Yes (0 violation)
6	438	1.130	5	9	4	Yes (0 violation)
7	670	-2.153	7	18	8	No (3 violations)
8	446	1.118	4	9	4	Yes (0 violation)
9	442	0.474	5	10	4	Yes (0 violation)
10	462	1.162	4	9	4	Yes (0 violation)
11	428	0.171	4	10	5	Yes (0 violation)
12	455	0.531	5	10	4	Yes (0 violation)
13	428	0.171	4	10	5	Yes (0 violation)

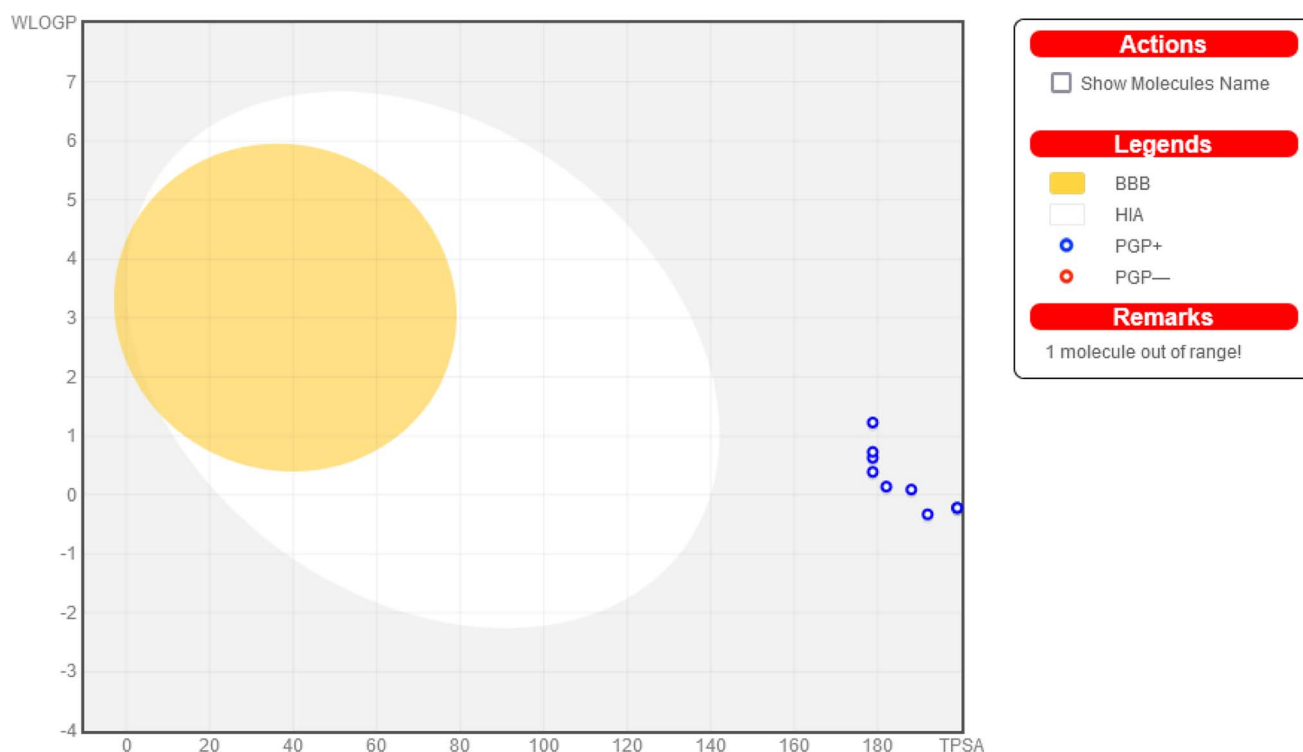


Fig. 3 Combined BOILED egg representation (created using Swiss ADME) of the studied compounds.

Table 5 Drug-likeness and toxicity predicted using OSIRIS property explorer

Pharmacodynamics					Pharmacokinetics				
Mutagenic	Tumorigenic	Eye and skin irritation	Reproductive effect		Solubility	Absorption	TPSA	Drug-likeness	Drug score
4	No	No	No	Medium	-4.76	-0.27	191.9	7.34	0.55
5	No	No	No	Medium	-5.42	0.89	178.7	7.15	0.47
6	No	No	No	Medium	-5.09	0.94	178.7	6.23	0.49
7	No	No	No	Medium	-6.11	-2.63	357.5	7.22	0.28
8	No	No	No	Medium	-5.81	1.15	178.7	7.64	0.43
9	No	No	No	Medium	-5.09	0.47	187.9	7.43	0.49
10	No	High	No	Medium	-6.68	1.74	178.7	7.03	0.22
11	No	No	No	Medium	-4.78	0.2	198.9	7.26	0.53
12	No	High	No	Medium	-5.11	0.44	182.0	6.25	0.29
13	No	No	No	Medium	-4.78	0.2	198.9	7.41	0.53



a notably low drug score, indicating potential limitations in its effectiveness as a drug candidate. Conversely, compounds **4**, **5**, **6**, **8**, **9**, **11**, and **13** demonstrate relatively favorable pharmacokinetic properties and drug scores, suggesting they may be more promising candidates for further development. These results emphasize the importance of comprehensive assessment of both pharmacodynamic and pharmacokinetic properties in evaluating the potential of compounds for drug development.

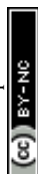
### 3.4. Molecular docking

The process of molecular docking involves the prediction of the optimal arrangement and strength of binding between a ligand (herein, the ten tested compounds **4**–**13**) and a receptor (herein,

the 5IKT molecule), resulting in the formation of a stable complex.<sup>63</sup> One of the receptors that has received a great deal of notice in recent years is 5IKT. The 5IKT receptor is the structure of tolafenamic acid bound to human cyclooxygenase2, which is an enzyme that catalyzes the synthesis of prostaglandins that are associated with inflammation and pain. Tolfenamic acid is a kind of nonsteroidal anti-inflammatory medication (NSAID) that prevents the enzyme cyclooxygenase from gaining accessibility to its target arachidonic acid.<sup>64,65</sup> Molecular docking may be used to create unique medicines targeting cyclooxygenase-2 in a substrate-selective manner, which means that they can selectively block the oxygenation of endocannabinoids, which are another class of substrates for cyclooxygenase-2, without affecting the oxygenation of arachidonic acid. This may have

**Table 6** Docking scores of the investigated compounds (from compound **4** to compound **13**) against 5IKT

	Ligand	Receptor	Interaction	Distance	<i>E</i> (kcal mol <sup>−1</sup> )	<i>S</i> (kcal mol <sup>−1</sup> )
<b>4</b>	C5	HIS 388	H-donor	3.45	−1.70	−8.82
	N8	HIS 388	H-donor	3.44	−2.40	
	O14	THR 212	H-acceptor	3.58	−0.70	
	6-ring	HIS 207	Pi-cation	3.59	−0.60	
<b>5</b>	N8	HIS 388	H-donor	3.44	−0.70	−7.67
	N20	GLN 454	H-acceptor	3.24	−2.50	
	6-ring	HIS 386	Pi-cation	3.37	−0.60	
	N23	GLN 454	H-donor	2.99	−1.60	
<b>6</b>	O11	HIS 207	H-acceptor	3.25	−0.90	−7.10
	N16	HIS 207	H-acceptor	3.01	−6.90	
	N20	ASN 382	H-acceptor	3.48	−1.20	
	6-ring	LEU 294	Pi-H	4.13	−0.70	
<b>7</b>	N12	ASP 213	H-donor	2.93	−5.30	−7.32
	O10	GLN 289	H-acceptor	3.51	−1.00	
	O13	LYS 215	H-acceptor	2.97	−5.90	
	O33	GLN 203	H-acceptor	3.21	−2.00	
<b>8</b>	N43	HIS 214	H-acceptor	3.20	−2.90	−7.46
	5-ring	HIS 207	Pi-cation	4.08	−0.80	
	C5	HIS 388	H-donor	3.53	−1.30	
	N8	HIS 388	H-donor	3.41	−8.70	
<b>9</b>	N13	ASN 382	H-donor	3.06	−0.90	−6.99
	O14	THR 212	H-acceptor	3.49	−1.10	
	6-ring	HIS 207	Pi-cation	3.83	−0.70	
	5-ring	LEU 294	Pi-H	4.22	−0.70	
<b>10</b>	6-ring	ILE 408	Pi-H	4.21	−0.60	−7.43
	N8	HIS 388	H-donor	3.04	−15.00	
	5-ring	HIS 207	Pi-cation	3.99	−0.90	
	6-ring	THR 212	Pi-H	3.62	−1.00	
<b>11</b>	6-ring	LEU 294	Pi-H	4.15	−0.80	−7.82
	N7	PHE 210	H-donor	3.42	−1.30	
	N23	TYR 385	H-donor	3.15	−0.70	
	N13	GLU 290	H-donor	3.08	−1.10	
<b>12</b>	N23	GLN 454	H-donor	3.17	−1.00	−7.76
	O30	HIS 388	H-donor	2.94	−11.80	
	O11	THR 212	H-acceptor	2.95	−2.70	
	O14	ASN 222	H-acceptor	3.03	−0.80	
<b>13</b>	N13	ALA 443	H-donor	3.16	−0.80	−7.37
	N23	ASN 382	H-donor	2.99	−1.00	
	5-ring	HIS 207	Pi-cation	3.22	−0.80	
	6-ring	THR 212	Pi-H	4.11	−0.70	
<b>13</b>	N13	TRP 387	H-donor	2.88	−1.30	−7.37
	O11	GLN 203	H-acceptor	3.24	−1.50	
	6-ring	GLN 203	Pi-H	3.63	−0.60	
	5-ring	HIS 207	Pi-cation	3.45	−2.30	



consequences for the design of new cyclooxygenase-2-targeting anti-inflammatory and analgesic medications. Therefore, the 5IKT receptor is important in molecular docking because it can provide structural information for designing new drugs that modulate the activity of cyclooxygenase-2 and its substrates. Overall, molecular docking is considered a powerful tool in exploring, discovering, and designing new drugs that can specifically target a certain enzyme.<sup>66</sup>

Here, the docking process was checked by re-docking and superimposition.<sup>51</sup> The re-docking procedure used the same procedures that had been used before. The re-docked 5IKT native ligand was found to be wholly overlaid on the native co-crystallized ligand (Fig. S1†). The re-docking and superimposition protocol gave good evidence for docking protocol validation.

Table 6 displays the docking scores of the examined compounds (4–13) against the 5IKT enzyme. The docking scores (*S*) exhibited a range between  $-8.82 \text{ kcal mol}^{-1}$  (for 4) and  $-6.99 \text{ kcal mol}^{-1}$  (for 9).

Compound 4 exhibited the highest activity with the most negative score among the compounds, with a value of  $-8.82 \text{ kcal mol}^{-1}$ . Following this, compound 12 displayed a score of  $-7.76 \text{ kcal mol}^{-1}$ , compound 5 had a score of  $-7.67 \text{ kcal mol}^{-1}$ , compound 8 had a score of  $-7.46 \text{ kcal mol}^{-1}$ , compound 10 had a score of  $-7.43 \text{ kcal mol}^{-1}$ , compound 13 had a score of  $-7.37 \text{ kcal mol}^{-1}$ , compound 7 had a score of  $-7.32 \text{ kcal mol}^{-1}$ , compound 6 had a score of  $-7.10 \text{ kcal mol}^{-1}$ , and finally compound 9 had a score of  $-6.99 \text{ kcal mol}^{-1}$ . Accordingly, compound 9 exhibited the lowest activity with the least negative score of  $-6.99 \text{ kcal mol}^{-1}$ . Fig. 4 illustrates the precise binding positions of the compounds under investigation inside the active site of the 5IKT interaction in both three-dimensional (3D) and two-dimensional (2D) representations. Additionally, Table 6 presents the docking data associated with these compounds.

In the examination of the molecular interactions in compound 4, it is shown that two H-donor and one H-acceptor bonds are established between C5 with HIS388, N8 with HIS388, and O14 with THR212, respectively, at distances of 3.45, 3.44, and 3.58 Å, respectively. Furthermore, it is seen that one pi-cation interaction was established between 6-ring with HIS207 at distance of 3.59 Å. These findings are listed in Table 6. In the instance of compound 11, three H-donors and two H-acceptor bonds are established between N13 with GLU290, N23 with GLN454, O30 with HIS388, O11 with THR212, and O14 with ASN222, respectively, at distances of 3.08, 3.17, 2.94, 2.95, and 3.03 Å, respectively. In compound 12, two hydrogen-donor bonds were observed, with distances of 3.16 and 2.99 Å, between N13 with ALA443 and N23 with ASN382, respectively (Table 6). Also, one pi-cation and one pi-H interactions were established between 5-ring with HIS207 and 6-ring with THR212 at 3.22 and 4.11 Å, respectively, as shown in Table 6.

### 3.5. Density functional theory (DFT) exploration

DFT calculations were performed to correlate the calculated HOMO–LUMO energy differences with the *in vitro* biological

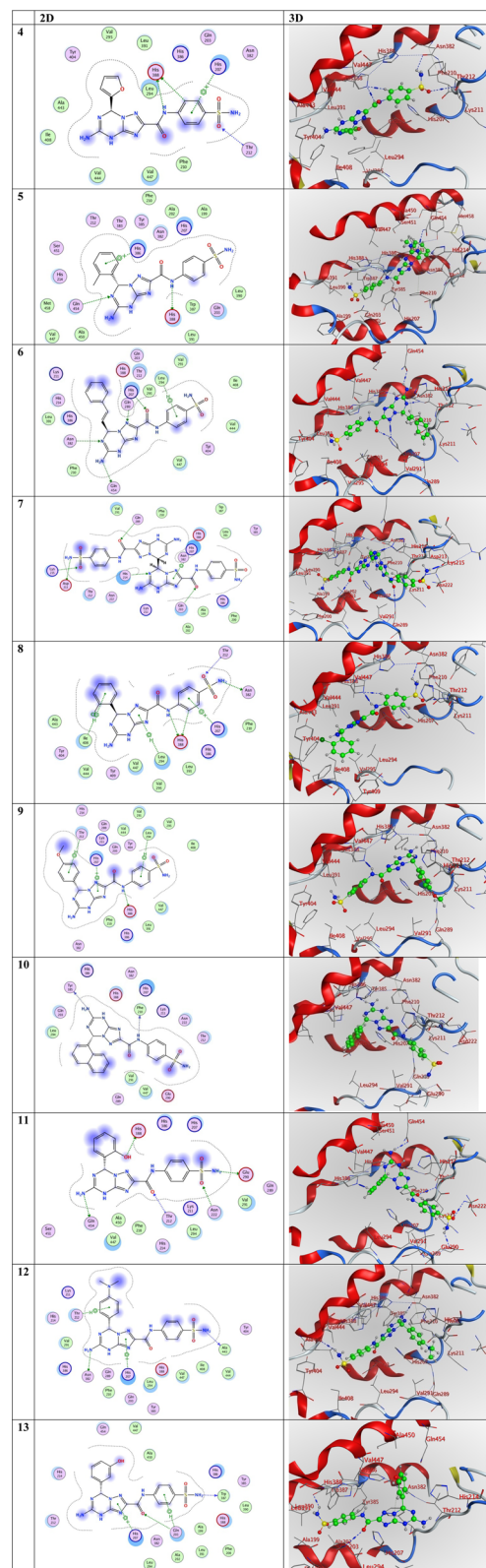


Fig. 4 3D and 2D representations of the molecular interactions of the investigated compounds (from compound 4 to compound 13) against the PDB ID: 5IKT.



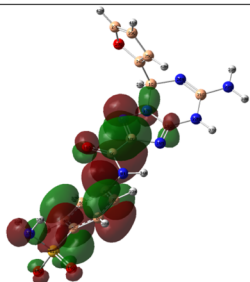
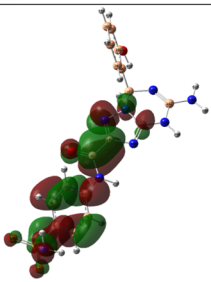
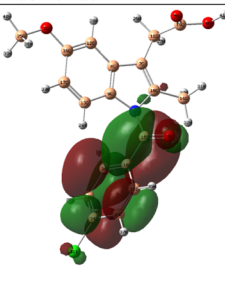
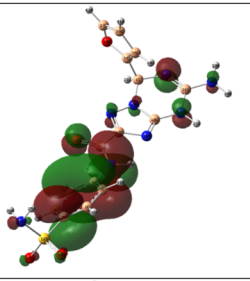
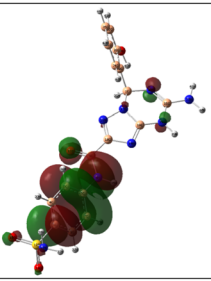
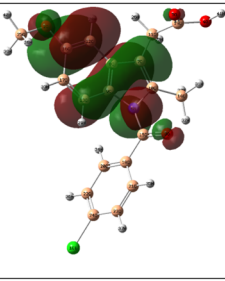
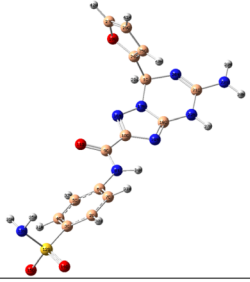
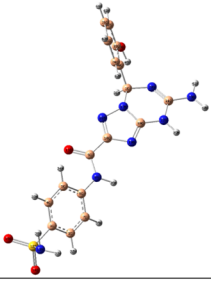
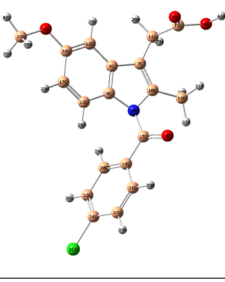
	4	11	Indomethacin
LUMO			
	$E_{\text{LUMO}} = -3.78 \text{ eV}$	$E_{\text{LUMO}} = -3.81 \text{ eV}$	$E_{\text{LUMO}} = -3.76 \text{ eV}$
	$\uparrow \Delta E = 2.43 \text{ eV}$	$\uparrow \Delta E = 2.18 \text{ eV}$	$\uparrow \Delta E = 2.95 \text{ eV}$
	$E_{\text{HOMO}} = -6.21 \text{ eV}$	$E_{\text{HOMO}} = -5.99 \text{ eV}$	$E_{\text{HOMO}} = -6.71 \text{ eV}$
HOMO			
	$\eta = 1.22 \text{ eV}$	$\eta = 1.09 \text{ eV}$	$\eta = 1.47 \text{ eV}$
	$\sigma = 0.82 \text{ eV}^{-1}$	$\sigma = 0.92 \text{ eV}^{-1}$	$\sigma = 0.68 \text{ eV}^{-1}$
3D			
	$\eta = 1.22 \text{ eV}$	$\eta = 1.09 \text{ eV}$	$\eta = 1.47 \text{ eV}$
	$\sigma = 0.82 \text{ eV}^{-1}$	$\sigma = 0.92 \text{ eV}^{-1}$	$\sigma = 0.68 \text{ eV}^{-1}$

Fig. 5 DFT exploration of compounds **4** and **11** and reference drug indomethacin.

activity results, looking for patterns or trends that may help explain the observed experimental outcomes.<sup>67</sup> Indomethacin was selected as it was used as the standard in the *in vitro* biological activity experiments. Considering the structural variations between the target compounds and indomethacin, we assess how these structural differences influence the electronic properties and reactivity and whether they can be linked to the biological activity.

The DFT investigation was explored *via* the B3LYP functional with the 6-311g(d,p) basis set. Fig. 5 displays the DFT assessments of the two highest-ranking compounds (**4** and **11**) obtained from the screening method and those of the reference drug indomethacin. The results of the DFT analysis demonstrated that the HOMO–LUMO energy differences ( $\Delta E$ ) of compounds **4** (2.43 eV) and **11** (2.18 eV) were lower than that of indomethacin (2.95 eV). This finding indicates the possibility and significance of molecular charge transfer.<sup>68–70</sup> Furthermore, the hardness ( $\eta$ , eV), and softness ( $\sigma$ , eV<sup>−1</sup>) values of the two highest-ranking compounds (**4** and **11**) identified by the screening approach, together with those of the reference drug indomethacin, were determined by evaluating the energies of their HOMO and LUMO orbitals using the Parr and Pearson

interpretation. Interestingly, compounds **4** and **5** had the highest chemical softness values (0.82 eV<sup>−1</sup> and 0.92 eV<sup>−1</sup>, respectively) and lowest chemical hardness values (1.22 eV and 1.09 eV, respectively) compared to those of indomethacin (0.68 eV<sup>−1</sup> and 1.47 eV, respectively), which might be responsible for the increased chemical reactivity compared to indomethacin.

## 4. Conclusion

The synthesis and characterization of new fused heterocyclic compounds based on purine analogues made from thio-carbohydrazide are reported in this study. The preparation method involved stirring conventionally in ethanol with drops of concentrated HCl. This is a simple process that provides high purities, high yields of triazolo-triazines with a sulfamoyl moiety, and the anticipated biological activity of the compounds. The molecular structures of the synthesized compounds were verified using spectroscopic methods and the compounds demonstrated highly significant anti-inflammatory activity. Particularly, compounds **4**, **5**, **8**, **11**, and **12** exhibited excellently effective RBC membrane stabilization, inhibition of protein denaturation, and inhibition of COX enzymes



compared to those of indomethacin. According to the *in vitro* anti-inflammatory activity, compounds **4**, **5**, **8**, **11** and **12** are promising as therapeutic candidates for treating inflammatory diseases. Careful and systematic plans could lead to further research employing innovative techniques and animal models. The COX inhibition study showed that these compounds exhibit remarkable COX-1/COX-2 inhibition, comparable with conventional indomethacin. COX 2 (PDB ID: 5IKT) was docked with the ten synthetic compounds (**4**–**13**). Compounds **4**, **11** and **12** had the highest binding affinity. The results suggest that these compounds inhibit COX 2 (PDB ID: 5IKT) and could be further studied for COX 2 targeting. DFT analysis was performed on the two most favorable compounds (**4** and **11**) identified through the screening methodology and the reference pharmaceutical agent indomethacin. The DFT analysis revealed that compounds **4** and **11** exhibited a reduced HOMO–LUMO energy difference in comparison to that of indomethacin. This discovery elucidates the potential importance of intermolecular charge transfer in this system.

## Animal rights

All animal procedures were performed in accordance with the Guidelines for Care and Use of Laboratory Animals of Sohag University and experiments were approved by the Animal Ethics Committee of “Committee for Scientific Research Ethics (CSRE) of Faculty of Science, Sohag University, Sohag, Egypt (protocol no. CSRE-26-23)”.

## Conflicts of interest

There are no conflicts to declare.

## References

- 1 N. Fujiwara and K. Kobayashi, Macrophages in inflammation, *Curr. Drug Targets: Inflammation Allergy*, 2005, **4**(3), 281–286.
- 2 D. A. Hume, The many alternative faces of macrophage activation, *Front. Immunol.*, 2015, **6**, 153172.
- 3 R. Kin, J. Notarte, T. Quimque, K. Macaranas, P. Adriel, V. Oliver, P. Hans, H. Arturo, I. V. Pilapil, M. Sophia, D. Tan, D. Q. Wei, W. Arlette, T. Deniz, Y. Chia-Hung, Ji. Seon, K. Gi-Young, C. Yung and M. Allan, *ACS Omega*, 2023, **8**(6), 5377–5392, DOI: [10.1021/acsomega.2c06451](https://doi.org/10.1021/acsomega.2c06451).
- 4 N. Ansari, F. Khodagholi, M. Ramin, M. Amini, H. Irannejad, L. Dargahi and A. D. Amirabad, Inhibition of LPS-induced apoptosis in differentiated-PC12 cells by new triazine derivatives through NF- $\kappa$ B-mediated suppression of COX-2, *Neurochem. Int.*, 2010, **57**(8), 958–968.
- 5 Q. Cao, X. Wang, L. Jia, A. K. Mondal, A. Diallo, G. A. Hawkins, S. K. Das, J. S. Parks, L. Yu and H. Shi, Inhibiting DNA methylation by 5-Aza-2'-deoxycytidine ameliorates atherosclerosis through suppressing macrophage inflammation, *Endocrinology*, 2014, **155**(12), 4925–4938.
- 6 L. Winand, S. Angela and N. Markus, Bioengineering of Antiinflammatory Natural Products, *ChemMedChem*, 2021, **16**(5), 767–776.
- 7 R. Kumar, T. Sirohi, H. Singh, R. Yadav, R. Roy, A. Chaudhary and S. Pandeya, 1, 2, 4-triazine analogs as novel class of therapeutic agents, *Mini-Rev. Med. Chem.*, 2014, **14**(2), 168–207.
- 8 O. A. Abd Allah, A. M. El-Saghier, A. M. Kadry and A. A. Seleem, Synthesis and Evaluation of Some Novel Curcumin Derivatives as Anti-inflammatory Agents, *Int. J. Pharm. Sci. Rev. Res.*, 2015, **32**(1), 87–92.
- 9 A. Tsar'kov, S. Smurov, E. Maevsky, I. Sedova, L. Bogdanova, V. Volsky and M. Kozhurin, Some Innovative Approaches To Maintaining The Adaptive Response Of The Organism Under Stress, *Mar. Med.*, 2018, **4**(1), 85–95.
- 10 M. Legraverend and D. S. Grierson, The purines: Potent and versatile small molecule inhibitors and modulators of key biological targets, *Biorg. Med. Chem.*, 2006, **14**(12), 3987–4006.
- 11 M. J. Perry and G. A. Higgs, Chemotherapeutic potential of phosphodiesterase inhibitors, *Curr. Opin. Chem. Biol.*, 1998, **2**(4), 472–481.
- 12 G. L. Russo, M. Russo and P. Ungaro, AMP-activated protein kinase: a target for old drugs against diabetes and cancer, *Biochem. Pharmacol.*, 2013, **86**(3), 339–350.
- 13 B. B. Fredholm, A. P. IJzerman, K. A. Jacobson, J. Linden and C. E. Müller, International Union of Basic and Clinical Pharmacology. LXXXI. Nomenclature and classification of adenosine receptors—an update, *Pharmacol. Rev.*, 2011, **63**(1), 1–34.
- 14 A. Bzowska, E. Kulikowska and D. Shugar, Purine nucleoside phosphorylases: properties, functions, and clinical aspects, *Pharmacol. Ther.*, 2000, **88**(3), 349–425.
- 15 A. K. Werner and C.-P. Witte, The biochemistry of nitrogen mobilization: purine ring catabolism, *Trends Plant Sci.*, 2011, **16**(7), 381–387.
- 16 A. Bloch, R. J. Leonard and C. A. Nichol, On the mode of action of 7-deaza-adenosine (tubercidin), *Biochim. Biophys. Acta, Nucleic Acids Protein Synth.*, 1967, **138**(1), 10–25.
- 17 R. M. McCarty and V. Bandarian, Deciphering deazapurine biosynthesis: pathway for pyrrolopyrimidine nucleosides toyocamycin and sangivamycin, *Chem. Biol.*, 2008, **15**(8), 790–798.
- 18 A. V. Dolzhenko, A. V. Dolzhenko and W. K. Chui, 1, 2, 4-triazolo [1, 5-a][1, 3, 5] triazines (5-azapurines): synthesis and biological activity, *Heterocycles*, 2006, **68**(8), 1723–1759.
- 19 R. Chovatiya and R. Medzhitov, Stress, inflammation, and defense of homeostasis, *Mol. Cell*, 2014, **54**(2), 281–288.
- 20 A. Dolzhenko, A. Dolzhenko and W. Chui, Pyrazolo [1, 5-a][1, 3, 5] triazines (5-aza-9-deazapurines): synthesis and biological activity, *Heterocycles*, 2008, **75**(7), 1575–1622.
- 21 S. R. Al-Ayash, T. H. Al-Noor and A. Abdou, Synthesis and Characterization of Metals Complexes with Uracil and Uracil Derivatives (A Review), *Russ. J. Gen. Chem.*, 2023, **93**(4), 987–995, DOI: [10.1134/S107036322304028X](https://doi.org/10.1134/S107036322304028X).
- 22 U. H. Hasan, A. M. Uttra and S. Rasool, Evaluation of in vitro and in vivo anti-arthritis potential of Berberis calliobotrys, *Bangladesh Journal of Pharmacology*, 2015, **10**(4), 807–819.



- 23 U. Shinde, A. Phadke, A. Nair, A. Mungantiwar, V. Dikshit and M. Saraf, Membrane stabilizing activity—a possible mechanism of action for the anti-inflammatory activity of Cedrus deodara wood oil, *Fitoterapia*, 1999, **70**(3), 251–257.
- 24 M. Murias, N. Handler, T. Erker, K. Pleban, G. Ecker, P. Saiko, T. Szekeres and W. Jäger, Resveratrol analogues as selective cyclooxygenase-2 inhibitors: synthesis and structure–activity relationship, *Biorg. Med. Chem.*, 2004, **12**(21), 5571–5578.
- 25 C. Scholz, S. Knorr, K. Hamacher and B. Schmidt, DOCKTITE A Highly Versatile Step-by-Step Workflow for Covalent Docking and Virtual Screening in the Molecular Operating Environment, *J. Chem. Inf. Model.*, 2015, **55**(2), 398–406.
- 26 A. Daina, O. Michielin and V. Zoete, SwissADME: a free web tool to evaluate pharmacokinetics, drug-likeness and medicinal chemistry friendliness of small molecules, *Sci. Rep.*, 2017, **7**(1), 42717.
- 27 N. Z. Ismail, N. Annamalai, N. N. M. Zain and H. Arsad, *J. Biol. Sci. Opin.*, 2020, **8**, 4–11.
- 28 A. M. Najjar, A. Eswayah, M. B. Moftah, M. K. R. Omar, E. Bobtaina, M. Najwa, T. A. Elhisadi, A. Tahani, S. M. Tawati, A. M. M. Khalifa, *et al.*, Rigidity and Flexibility of Pyrazole, s-Triazole, and v-Triazole Derivative of Chloroquine as Potential Therapeutic against COVID-19, *J. Med. Chem. Sci.*, 2023, **6**(9), 2056–2084, DOI: [10.26655/jmchemsci.2023.9.14](https://doi.org/10.26655/jmchemsci.2023.9.14).
- 29 S. Shaaban, Y. S. Al-Faiyz, G. M. Alsulaim, M. Alaasar, N. Amri, H. Ba-Ghazal, A. A. Al-Karmalawy and A. Abdou, Synthesis of new organoselenium-based succinilic and maleanilic derivatives and in silico studies as possible SARS-CoV-2 main protease inhibitors, *Inorganics*, 2023, **11**(8), 321.
- 30 B. J. Orlando and M. G. Malkowski, Substrate-selective inhibition of cyclooxygenase-2 by fenamic acid derivatives is dependent on peroxide tone, *J. Biol. Chem.*, 2016, **291**(29), 15069–15081.
- 31 T. Murugan, R. Venkatesh, K. Geetha and A. Abdou, Synthesis, spectral investigation, DFT, antibacterial, antifungal and molecular docking studies of Ni (II), Zn (II), Cd (II) complexes of tetradentate Schiff-base ligand, *Asian J. Chem.*, 2023, **35**, 1509–1517.
- 32 H. M. Abd El-Lateef, M. M. Khalaf, A. A. Amer, M. Kandeel, A. A. Abdelhamid and A. Abdou, Synthesis, characterization, antimicrobial, density functional theory, and molecular docking studies of novel Mn (II), Fe (III), and Cr (III) complexes incorporating 4-(2-hydroxyphenyl azo)-1-naphthol (Az), *ACS Omega*, 2023, **8**(29), 25877–25891.
- 33 K. R. Valasani, J. R. Vangavaragu, V. W. Day and S. S. Yan, Structure based design, synthesis, pharmacophore modeling, virtual screening, and molecular docking studies for identification of novel cyclophilin D inhibitors, *J. Chem. Inf. Model.*, 2014, **54**(3), 902–912.
- 34 E. M. Terefe and A. Ghosh, Molecular docking, validation, dynamics simulations, and pharmacokinetic prediction of phytochemicals isolated from Croton dichogamus against the HIV-1 reverse transcriptase, *Bioinf. Biol. Insights*, 2022, **16**, 11779322221125605.
- 35 K. E. Hevener, W. Zhao, D. M. Ball, K. Babaoglu, J. Qi, S. W. White and R. E. Lee, Validation of molecular docking programs for virtual screening against dihydropteroate synthase, *J. Chem. Inf. Model.*, 2009, **49**(2), 444–460.
- 36 A. D. Becke, Density-functional exchange-energy approximation with correct asymptotic behavior, *Phys. Rev. A: At., Mol., Opt. Phys.*, 1988, **38**(6), 3098.
- 37 M. A. E. A. A. El-Remaily, O. Elhady, A. Abdou, D. Alhashmialameer, T. N. A. Eskander and A. M. Abu-Dief, Development of new 2-(Benzothiazol-2-ylimino)-2,3-dihydro-1H-imidazole-4-ol complexes as a robust catalysts for synthesis of thiazole 6-carbonitrile derivatives supported by DFT studies, *J. Mol. Struct.*, 2023, **1292**, 136188, DOI: [10.1016/j.molstruc.2023.136188](https://doi.org/10.1016/j.molstruc.2023.136188).
- 38 C. Lee, W. Yang and R. G. Parr, Development of the Colle-Salvetti correlation-energy formula into a functional of the electron density, *Phys. Rev. B: Condens. Matter Mater. Phys.*, 1988, **37**(2), 785.
- 39 J. A. Plumley and J. Dannenberg, A comparison of the behavior of functional/basis set combinations for hydrogen-bonding in the water dimer with emphasis on basis set superposition error, *J. Comput. Chem.*, 2011, **32**(8), 1519–1527.
- 40 A. Tomberg, Gaussian 09w tutorial, *An Introduction to Computational Chemistry Using G09W and Avogadro Software*, 2013, pp. 1–36.
- 41 A. Abdou, O. A. Omran, J. H. Al-Fahemi, R. S. Jassas, M. M. Al-Rooqi, E. M. Hussein, Z. Moussa and S. A. Ahmed, Lower rim thiocalixarenes derivatives incorporating multiple coordinating carbonyl groups: Synthesis, characterization, ion-responsive ability and DFT computational analysis, *J. Mol. Struct.*, 2023, **1293**, 136264, DOI: [10.1016/j.molstruc.2023.136264](https://doi.org/10.1016/j.molstruc.2023.136264).
- 42 N. A. Elkanzi, A. M. Kadry, R. M. Ryad, R. B. Bakr, M. A. E. A. Ali El-Remaily and A. M. Ali, Efficient and recoverable bio-organic catalyst cysteine for synthesis, docking study, and antifungal activity of new bio-active 3, 4-dihydropyrimidin-2 (1 H)-ones/thiones under microwave irradiation, *ACS Omega*, 2022, **7**(26), 22839–22849.
- 43 A. M. El-Saghier, A. Abdul-Baset, O. M. El-Hady and A. M. Kadry, Synthesis of some new thiadiazole/thiadiazine derivatives as potent biologically active compounds, *Sohag J. Sci.*, 2023, **8**(3), 371–375.
- 44 A. M. El-Saghier, S. S. Enaili, A. Abdou, A. M. Hamed and A. M. Kadry, An operationally simple, one-pot, convenient synthesis, and in vitro anti-inflammatory activity of some new spirotriazolotriazine derivatives, *J. Heterocycl. Chem.*, 2024, **61**(1), 146–162.
- 45 O. A. Abd Allah, A. M. El-Saghier and A. M. Kadry, Synthesis, structural stability calculation, and antibacterial evaluation of novel 3, 5-diphenylcyclohex-2-en-1-one derivatives, *Synth. Commun.*, 2015, **45**(8), 944–957.
- 46 A. H. Abdelmonsef, A. M. El-Saghier and A. M. Kadry, Ultrasound-assisted green synthesis of triazole-based azomethine/thiazolidin-4-one hybrid inhibitors for cancer therapy through targeting dysregulation signatures of some Rab proteins, *Green Chem. Lett. Rev.*, 2023, **16**(1), 2150394.



- 47 A. M. El-Saghier, M. A. Mohamed, O. A. Abdalla and A. M. Kadry, Utility of amino acid coupled 1,2,4-triazoles in organic synthesis: synthesis of some new antileishmanial agents, *Bull. Chem. Soc. Ethiop.*, 2018, **32**(3), 559–570, DOI: [10.4314/bcse.v32i3.14](#).
- 48 M. A. Mohamed, A. M. Kadry, S. A. Bekhit, M. A. S. Abourehab, K. Amagase, T. M. Ibrahim and A. A. Bekhit, Spiro heterocycles bearing piperidine moiety as potential scaffold for antileishmanial activity: synthesis, biological evaluation, and in silico studies, *J. Enzyme Inhib. Med. Chem.*, 2023, **38**(1), 330–342, DOI: [10.1080/14756366.2022.215076](#).
- 49 A. M. El-Saghier, S. S. Enaili, A. Abdou and A. M. Kadry, An efficient eco-friendly, simple, and green synthesis of some new spiro-N-(4-sulfamoyl-phenyl)-1, 3, 4-thiadiazole-2-carboxamide derivatives as potential inhibitors of SARS-CoV-2 proteases: drug-likeness, pharmacophore, molecular docking, and DFT exploration, *Mol. Diversity*, 2023, 1–22.
- 50 A. M. El-Saghier, A. Abdou, M. A. Mohamed, H. M. Abd El-Lateef and A. M. Kadry, Novel 2-acetamido-2-ylidene-4-imidazole derivatives (El-Saghier reaction): Green synthesis, biological assessment, and molecular docking, *ACS Omega*, 2023, **8**(33), 30519–30531.
- 51 A. M. El-Saghier, S. S. Enaili, A. M. Kadry, A. Abdou and M. A. Gad, Green synthesis, biological and molecular docking of some novel sulfonamide thiadiazole derivatives as potential insecticidal against *Spodoptera littoralis*, *Sci. Rep.*, 2023, **13**(1), 19142.
- 52 M. A. Mohamed, A. A. Bekhit, O. A. Abd Allah, A. M. Kadry, T. M. Ibrahim, S. A. Bekhit, A. Kikuko and A. M. El-Saghier, Synthesis and antimicrobial activity of some novel 1,2-dihydro-[1,2,4]triazolo[1,5-a]pyrimidines bearing amino acid moiety, *RSC Adv.*, 2021, **11**, 2905–2916.
- 53 J. C. Maroon, J. W. Bost and A. Maroon, Natural anti-inflammatory agents for pain relief, *Surg. Neurol. Int.*, 2010, **1**, 80–87.
- 54 S. Hariforoosh, W. Asghar and F. Jamali, Adverse effects of nonsteroidal antiinflammatory drugs: an update of gastrointestinal, cardiovascular and renal complications, *J. Pharm. Pharm. Sci.*, 2013, **16**(5), 821–847.
- 55 H. ur Rashid, Y. Xu, N. Ahmad, Y. Muhammad and L. Wang, Promising anti-inflammatory effects of chalcones via inhibition of cyclooxygenase, prostaglandin E2, inducible NO synthase and nuclear factor  $\kappa$ b activities, *Bioorg. Chem.*, 2019, **87**, 335–365.
- 56 G. Yuan, M. L. Wahlqvist, G. He, M. Yang and D. Li, Natural products and anti-inflammatory activity, *Asia Pac. J. Clin. Nutr.*, 2006, **15**(2), 143–152.
- 57 Y. Ju and R. S. Varma, Aqueous N-heterocyclization of primary amines and hydrazines with dihalides: microwave-assisted syntheses of N-azacycloalkanes, isoindole, pyrazole, pyrazolidine, and phthalazine derivatives, *J. Org. Chem.*, 2006, **71**(1), 135–141.
- 58 L. Winand, A. Sester and M. Nett, Bioengineering of anti-inflammatory natural products, *ChemMedChem*, 2021, **16**(5), 767–776.
- 59 M. García-Valverde and T. Torroba, *Sulfur-nitrogen Heterocycles*, 2005, vol. 10, pp. 318–320.
- 60 X.-Y. Meng, H.-X. Zhang, M. Mezei and M. Cui, Molecular docking: a powerful approach for structure-based drug discovery, *Curr. Comput.-Aided Drug Des.*, 2011, **7**(2), 146–157.
- 61 C. A. Lipinski, F. Lombardo, B. W. Dominy and P. J. Feeney, Experimental and computational approaches to estimate solubility and permeability in drug discovery and development settings, *Adv. Drug Delivery Rev.*, 1997, **23**(1–3), 3–25.
- 62 A. Daina and V. Zoete, A boiled-egg to predict gastrointestinal absorption and brain penetration of small molecules, *ChemMedChem*, 2016, **11**(11), 1117–1121.
- 63 H. M. Abd El-Lateef, M. M. Khalaf, M. Kandeel and A. Abdou, Synthesis, Characterization, DFT, Biological and Molecular Docking of Mixed Ligand Complexes of Ni(II), Co(II), and Cu(II) Based on Ciprofloxacin and 2-(1H-benzimidazol-2-yl) phenol, *Inorg. Chem. Commun.*, 2023, **155**, 111087, DOI: [10.1016/j.inoche.2023.111087](#).
- 64 L. Pinzi and G. Rastelli, Molecular docking: shifting paradigms in drug discovery, *Int. J. Mol. Sci.*, 2019, **20**(18), 4331.
- 65 H. M. Abd El-Lateef, M. M. Khalaf, F. El-Taib Heakal and A. Abdou, Fe(III), Ni(II), and Cu(II)-moxifloxacin-tri-substituted imidazole mixed ligand complexes: Synthesis, structural, DFT, biological, and protein-binding analysis, *Inorg. Chem. Commun.*, 2023, **158**, 111486, DOI: [10.1016/j.inoche.2023.111486](#).
- 66 H. M. Abd El-Lateef, A. M. Ali, M. M. Khalaf and A. Abdou, New iron (III), cobalt (II), nickel (II), copper (II), zinc (II) mixed-ligand complexes: Synthesis, structural, DFT, molecular docking and antimicrobial analysis, *Bull. Chem. Soc. Ethiop.*, 2024, **38**(1), 147–166.
- 67 R. K. Mohapatra, A. Mahal, A. Ansari, M. Kumar, J. P. Guru, A. K. Sarangi, A. Abdou, S. Mishra, M. Aljeldah, B. M. AlShehail, *et al.*, Comparison of the binding energies of approved mpox drugs and phytochemicals through molecular docking, molecular dynamics simulation, and ADMET studies: An in silico approach, *J. Biosaf. Biosecur.*, 2023, **5**(3), 118–132, DOI: [10.1016/j.jobbb.2023.09.001](#).
- 68 R. G. Pearson, The HSAB principle—more quantitative aspects, *Inorg. Chim. Acta*, 1995, **240**(1–2), 93–98.
- 69 A. M. El-Saghier, H. F. Abd El-Halim, L. H. Abdel-Rahman and A. Kadry, Green Synthesis of new Trizole Based Heterocyclic Amino Acids Ligands and their Transition Metal Complexes. Characterization, Kinetics, Antimicrobial and Docking Studies, *Appl. Organomet. Chem.*, 2019, **33**, e4641, DOI: [10.1002/aoc.464118](#).
- 70 M. A. E. A. A. El-Remaily, T. El-Dabea, R. M. El-Khatib, A. Abdou, M. A. El Hamd and A. M. Abu-Dief, Efficiency and development of guanidine chelate catalysts for rapid and green synthesis of 7-amino-4,5-dihydro-tetrazolo[1,5-a]pyrimidine-6-carbonitrile derivatives supported by density functional theory (DFT) studies, *Appl. Organomet. Chem.*, 2023, **37**(11), e7262, DOI: [10.1002/aoc.7262](#).

